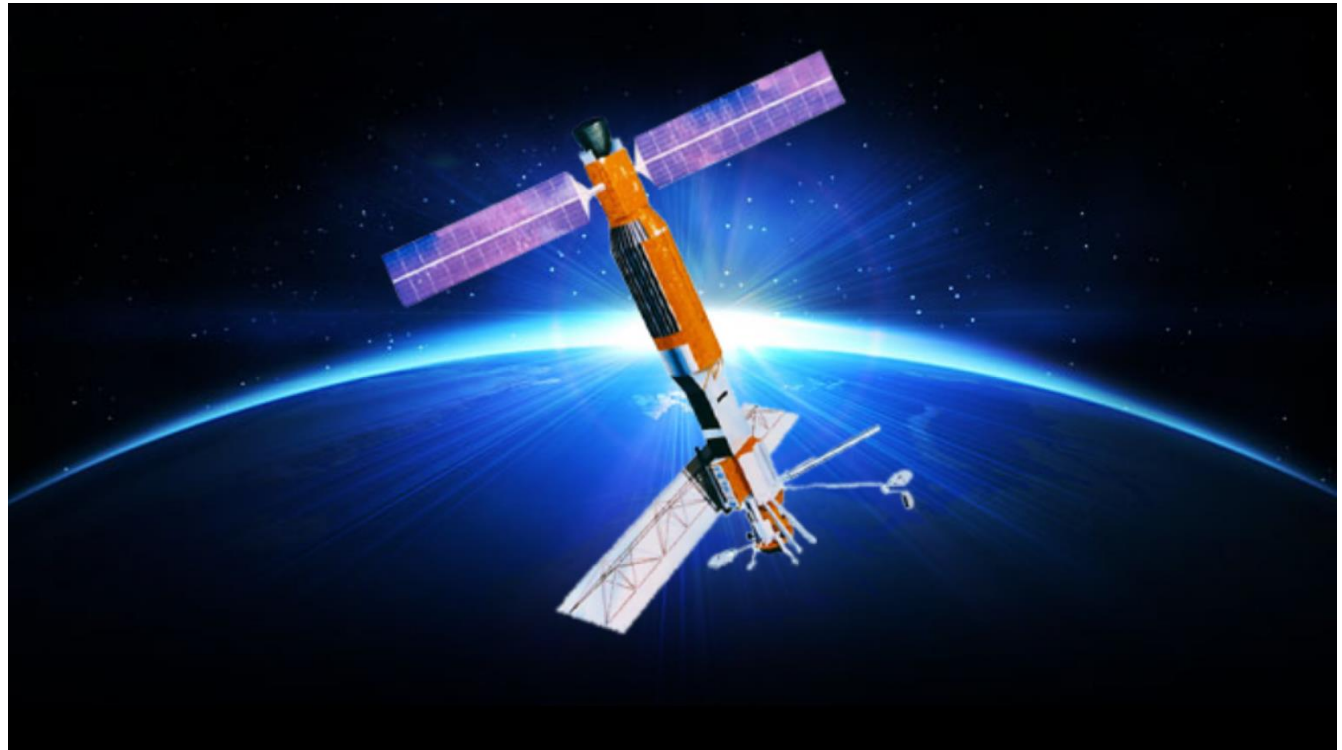


Internal Identifier: EITRM106937:
AMICOS Training Material set 2:
SAR Interferometry theory and
applications



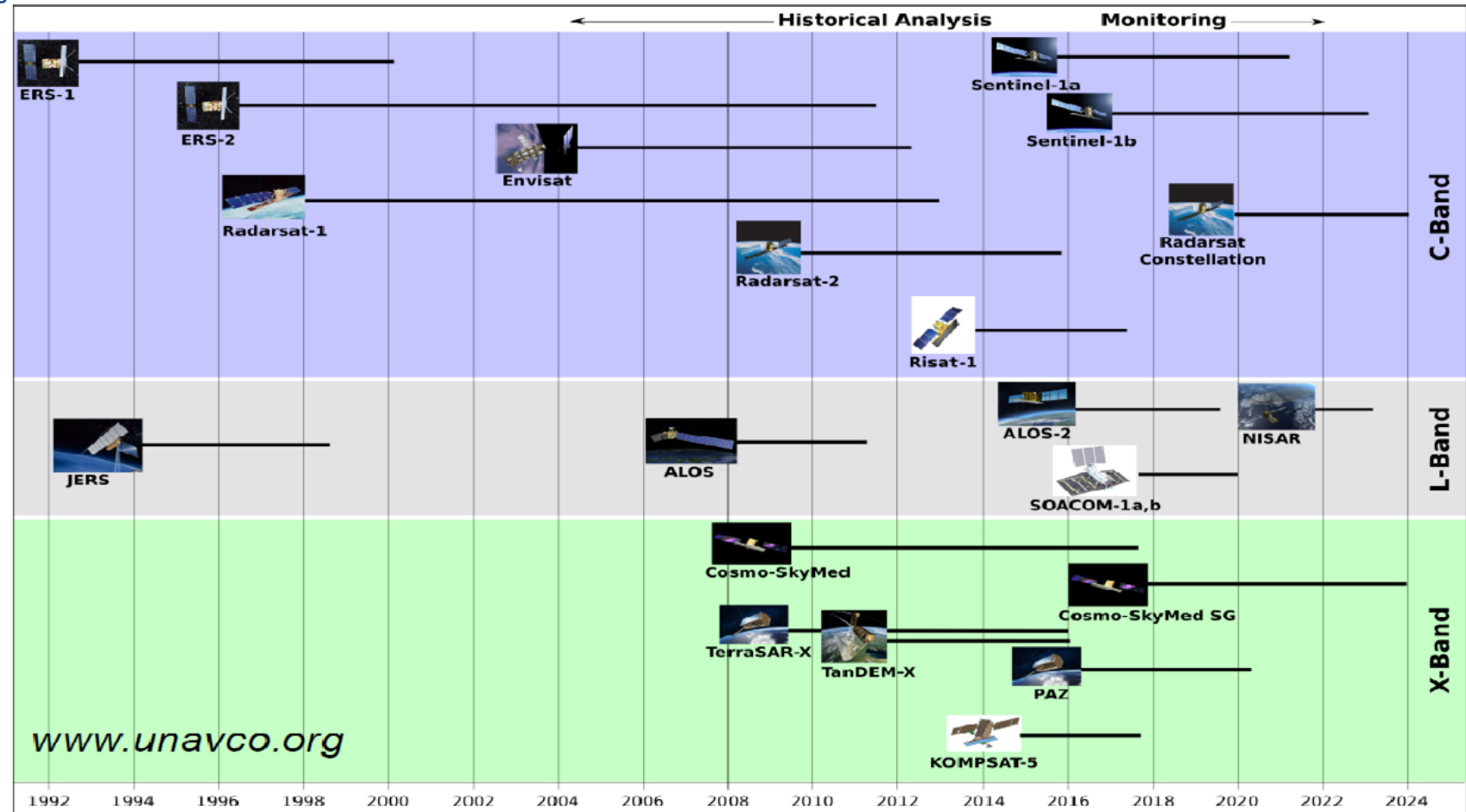
About 40 years of SAR missions...

- The history of civilian satellite SAR systems began with the 1978 NASA Seasat satellite, which was the first satellite equipped with a SAR sensor, operating at L band (24 cm of wavelength) of the electromagnetic spectrum.
- The mission was designed for remote sensing of the Earth's oceans to demonstrate the feasibility of global satellite monitoring of oceanographic phenomena and to help determine the requirements for an operational ocean remote sensing satellite system



About 40 years of SAR missions...

- Continuous performance improvement;
- Multifrequency (X- C- L-band);
- Low sampling revisiting time (from 35 dd to 1-2 dd) thanks to constellations;
- Different line of sights (from 23° up to >50°);
- Multi acquisitions mode (Sentinel-1, ALOS-2, etc.).



New Generation ESA SAR: the Sentinel-1



RawMaterials

Connecting matters

Launch: 3 April 2014

Orbit: Polar, Sun-synchronous at an altitude of 693 km

Revisit time: 12 days, 6 days with the second satellite, since 2015

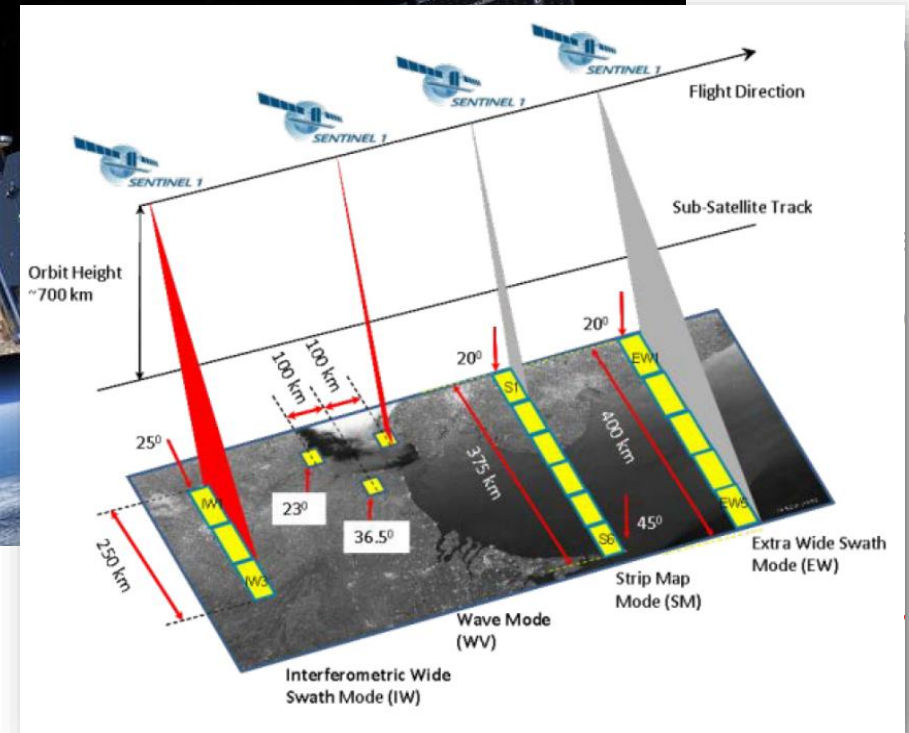
Life: Minimum of seven years

Instrument: C-band SAR at 5.405 GHz, with dual pol capability

4 Operational modes:

- Interferometric wide-swath mode at 250 km and 5×20 m resolution
- Wave-mode images of 20×20 km and 5×5 m resolution (at 100 km intervals)
- Strip map mode at 80 km swath and 5×5 m resolution
- Extra wide-swath mode of 400 km and 20×40 m resolution

Main applications: Monitoring sea ice, oil spills, marine winds & waves, land-use change, land deformation among others, and to respond to emergencies such as floods and earthquakes



This activity has received funding from the European Institute of Innovation and Technology (EIT), a body of the European Union, under the Horizon 2020, the EU Framework Programme for Research and Innovation

SAR Interferometry (InSAR) theory



InSAR technique indicates the pixel to pixel phase difference between two SAR images of the same scene viewed from comparable geometries.

We call *interferogram* the image of the pixel to pixel phase difference.

Whenever the surface backscattering is unchanged (high coherence), the phase component of each pixel contains the satellite to target distance (R):



This activity has received funding from the European Institute of Innovation and Technology (EIT), a body of the European Union, under the Horizon 2020, the EU Framework Programme for Research and Innovation

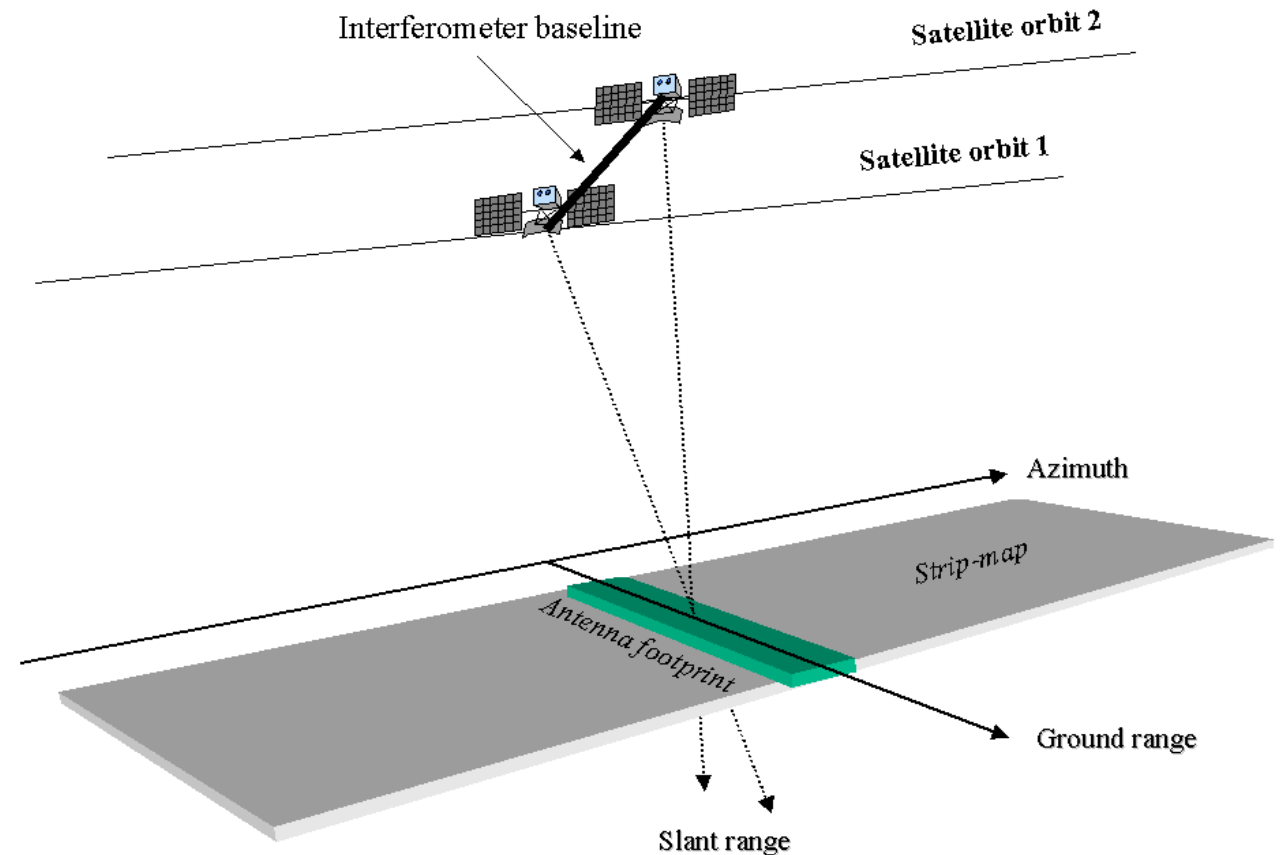


SAR Interferometry (InSAR)

Two radar antennas (1 and 2) observe a target with a slight separation in space, the interferometric *baseline*.

B_p is the parallel baseline

B_n is the normal baseline

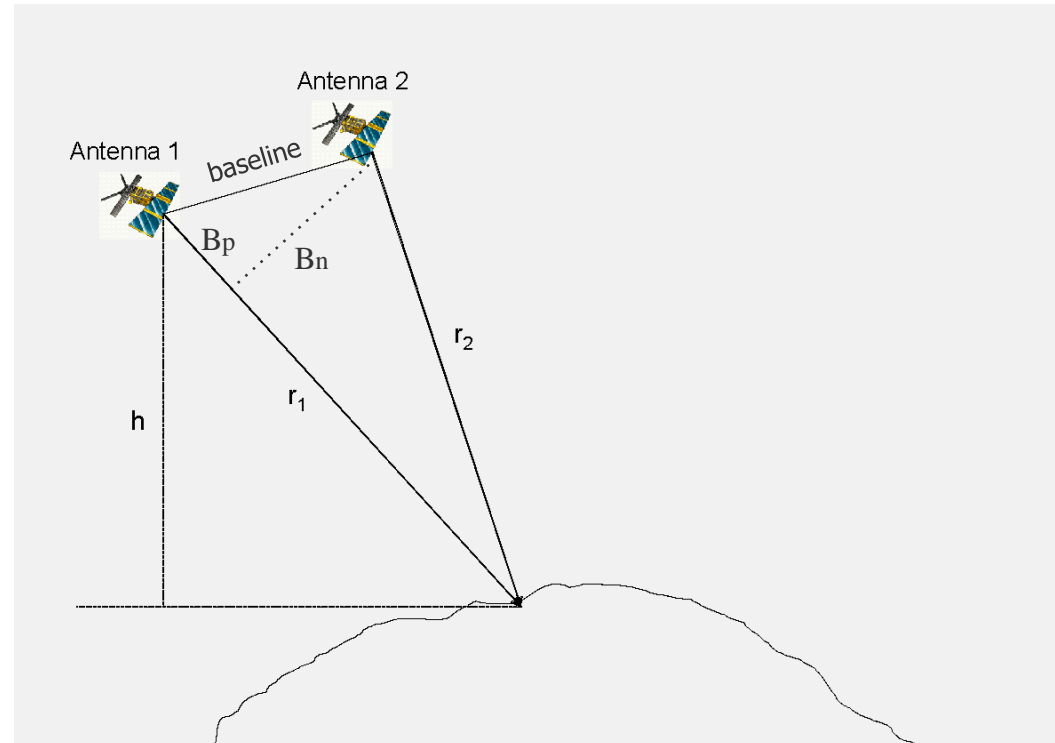


SAR Interferometry (InSAR)

Two radar antennas (1 and 2) observe a target with a slight separation in space, the interferometric *baseline*.

B_p is the parallel baseline

B_n is the normal baseline



If the two images are acquired simultaneously **single-pass interferometry**

If the two images are acquired at different times **repeat-pass**

interferometry



SAR Interferometry (InSAR)

Be S_1 and S_2 the received signals at two satellite positions:

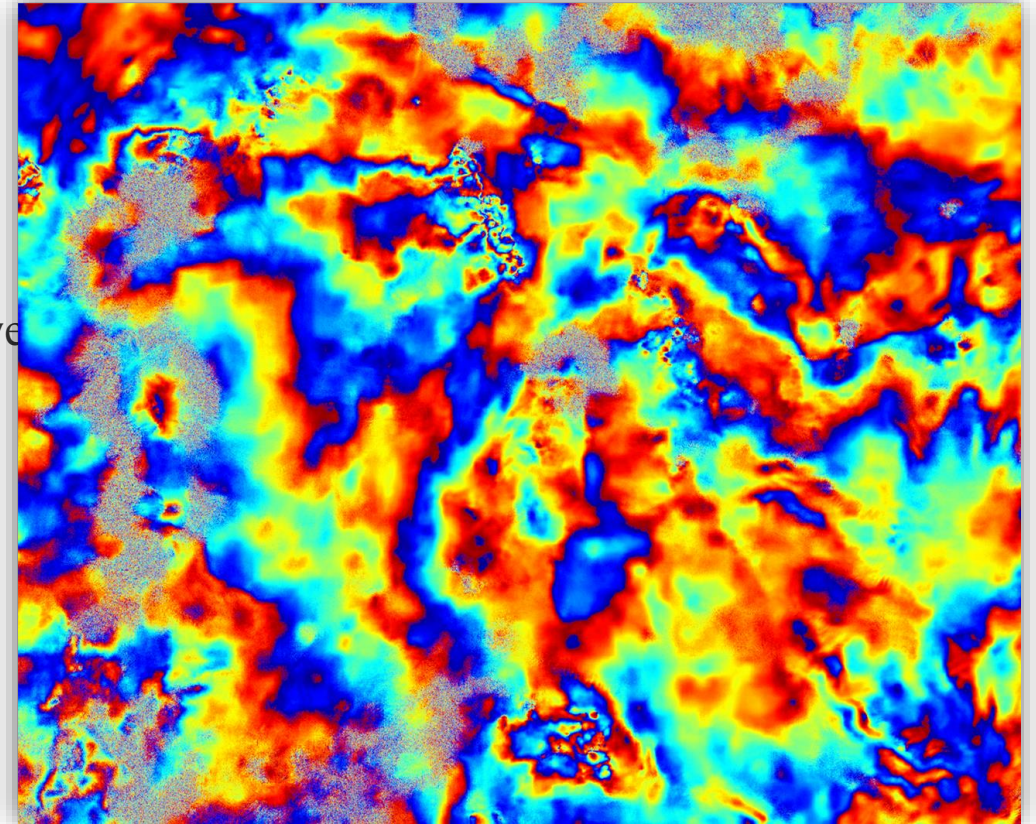
$$S_1 = A_1 e^{-j\phi_1} = A_1 e^{-j\frac{4\pi}{\lambda}r_1}$$

$$S_2 = A_2 e^{-j\phi_2} = A_2 e^{-j\frac{4\pi}{\lambda}r_2}$$

The *interferogram* is the map of the pixel-to-pixel phase difference between S_1 and S_2 :

$$S_1 S_2^* = A_1 A_2 e^{-j\frac{4\pi}{\lambda}(r_1 - r_2)}$$

In the explicit form above the relation phase-distance is manifest.



SAR Interferometry (InSAR)



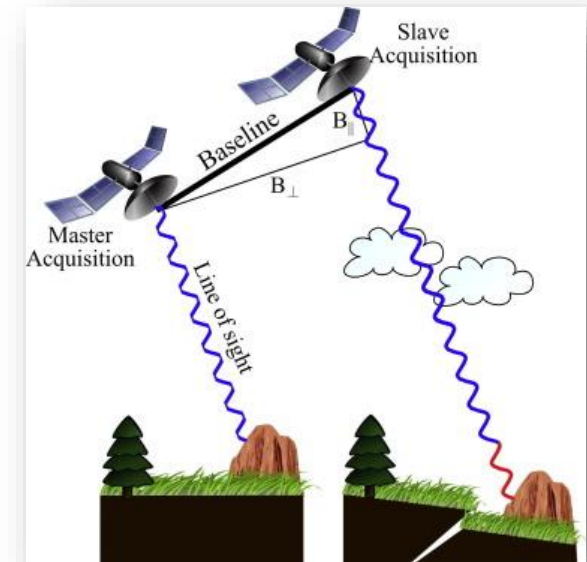
RawMaterials

Connecting matters

The interferometric phase contains some distinct contributions:

$$\varphi_{int} = \varphi_{flat} + \varphi_{topo} + \varphi_{atm} + \varphi_{err} + \varphi_{displ}$$

φ_f	flat Earth	→	removable
φ_{topo}	topographic phase	→	removable
φ_{atm}	atmospheric phase	→	not removable with standard techniques
φ_{err}	noise (error phase)	→	not removable
φ_{displ}	deformation phase	→	I'm interested in

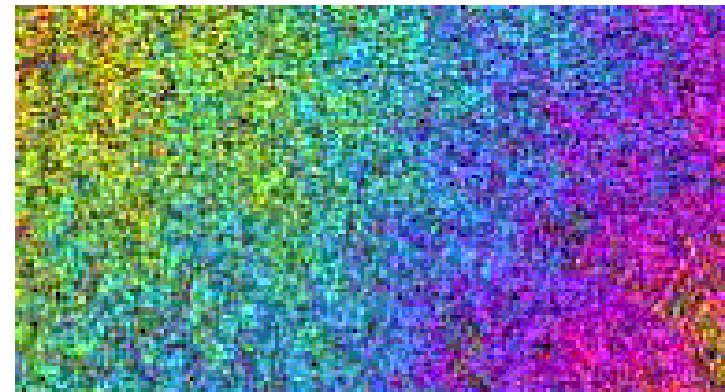
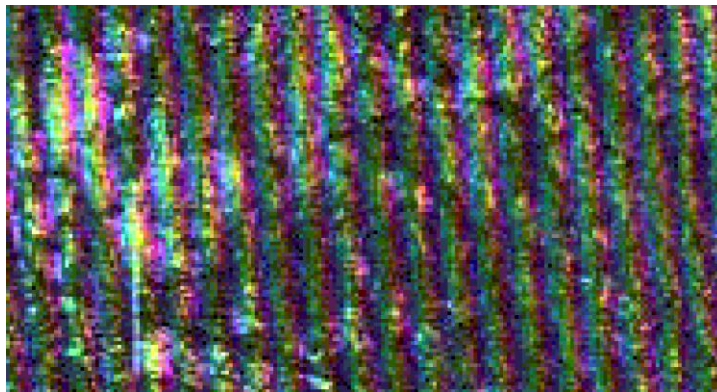
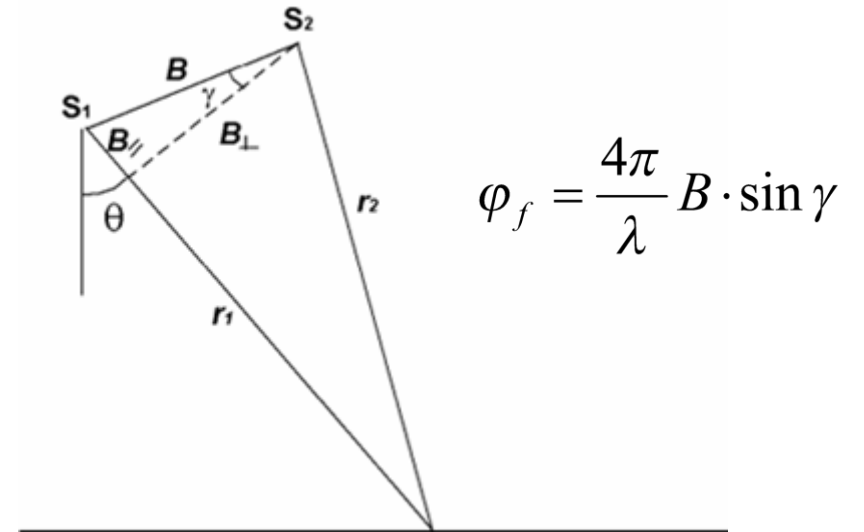


This activity has received funding from the European Institute of Innovation and Technology (EIT), a body of the European Union, under the Horizon 2020, the EU Framework Programme for Research and Innovation

Supported by:  RawMaterials
Connecting matters

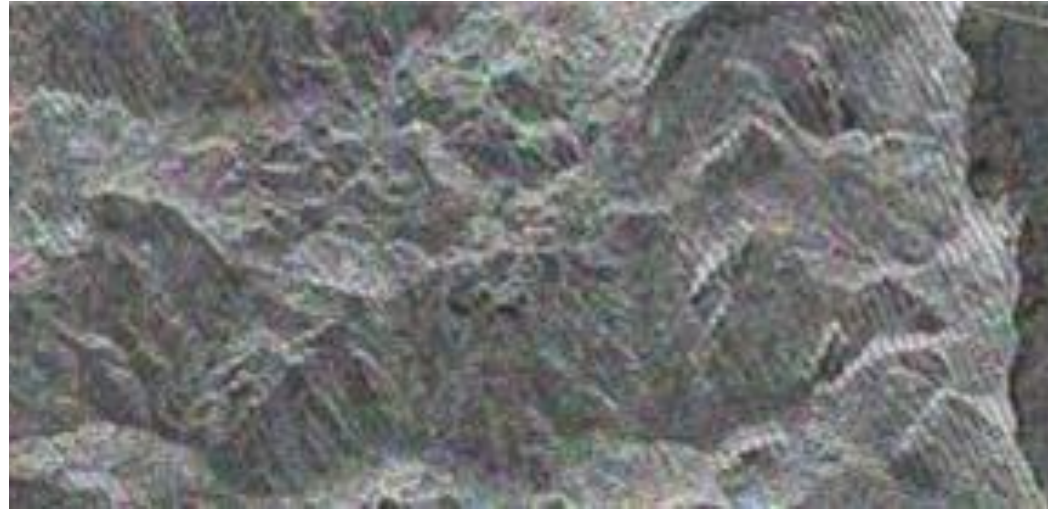
Flat Earth

- Raw interferogram includes a quasi-linear phase trend caused by tilt of terrain surface relative to the baseline
- Flattening removes interferometric phase modeled using a sphere with radius of curvature derived from the ellipsoid

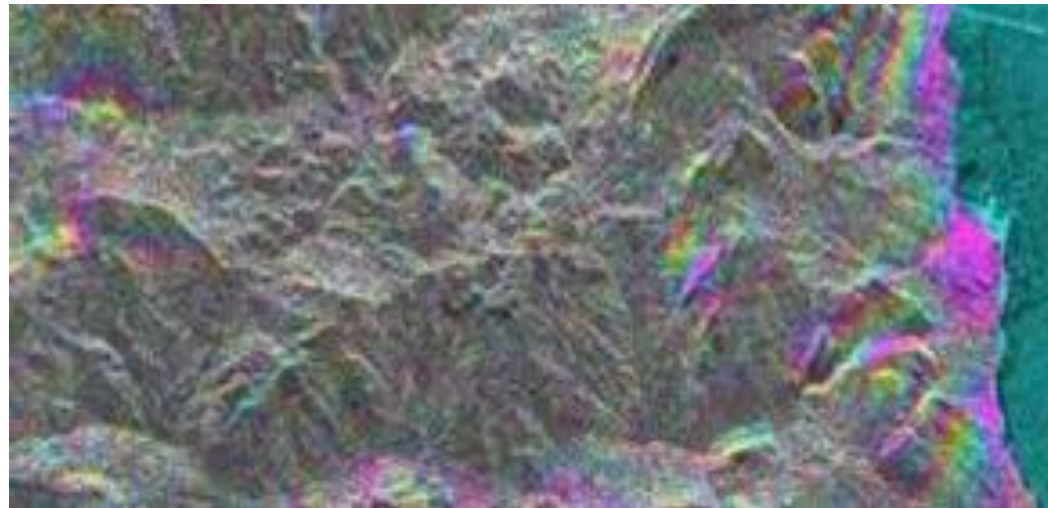


Flat Earth

Unflattened interferogram



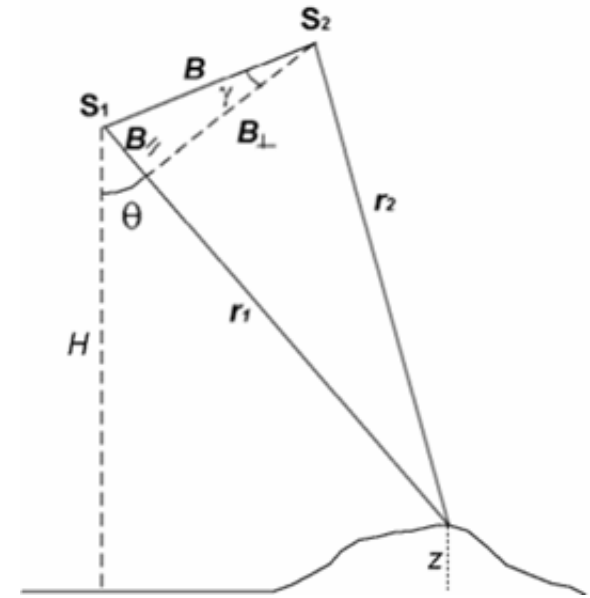
Flattened interferogram



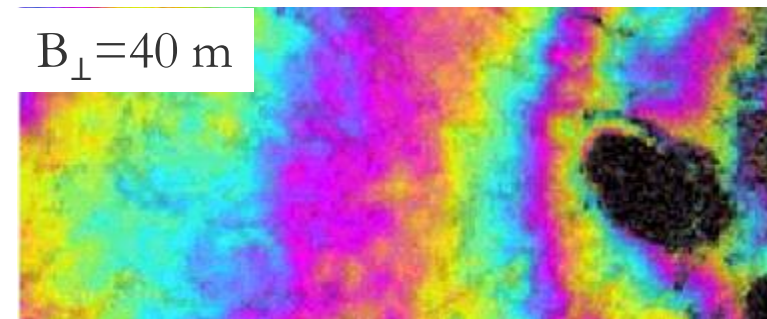
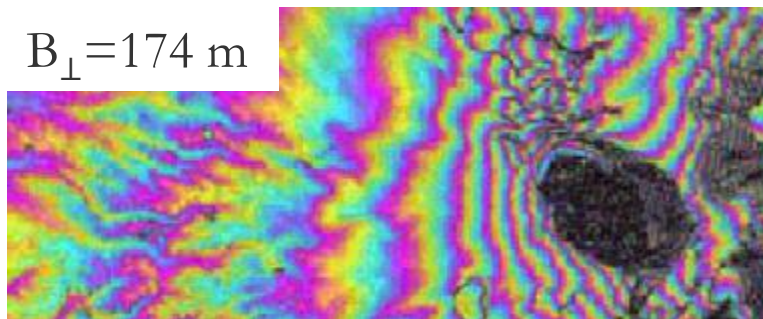
Topographic phase

The topographic phase contains the information relative to the relief. The spacing between the fringes depends on the perpendicular baseline: the longer the perpendicular baseline, the narrower the fringes

$$\frac{4\pi}{\lambda} (r_2 - r_1) \cong -\frac{4\pi}{\lambda} B \cdot \sin \gamma - \frac{4\pi}{\lambda} B_{\perp} \cdot \frac{z}{r_1 \sin \vartheta} = \varphi_f + \varphi_{topo}$$



$$H \cong z - r_1 \sin \vartheta$$

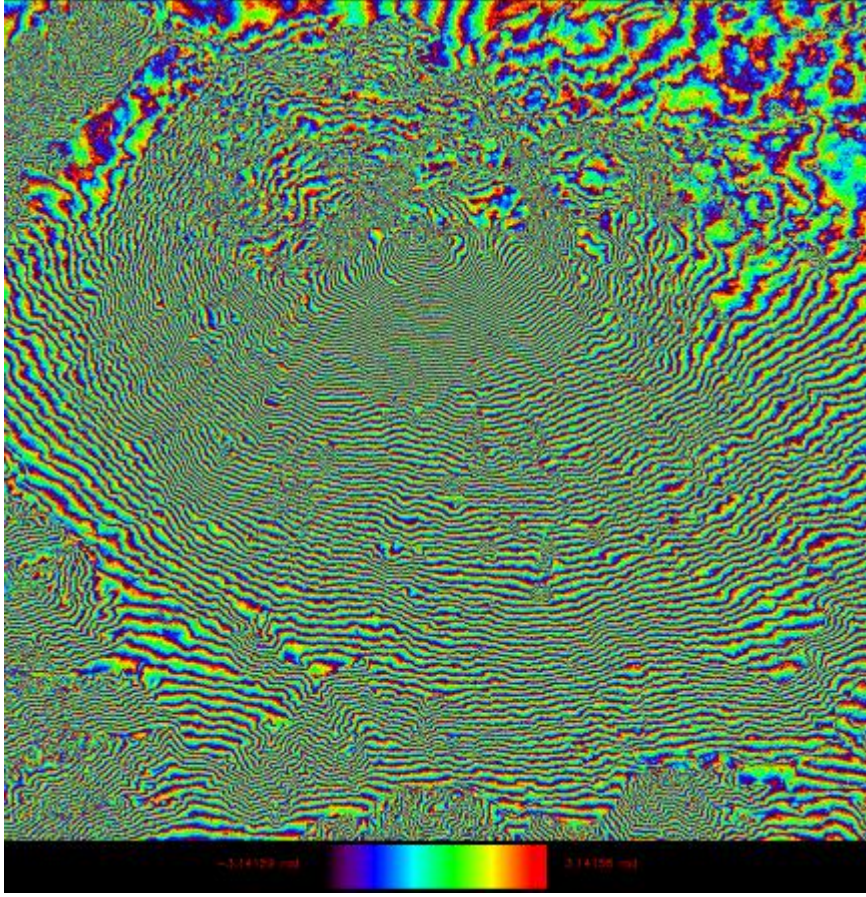
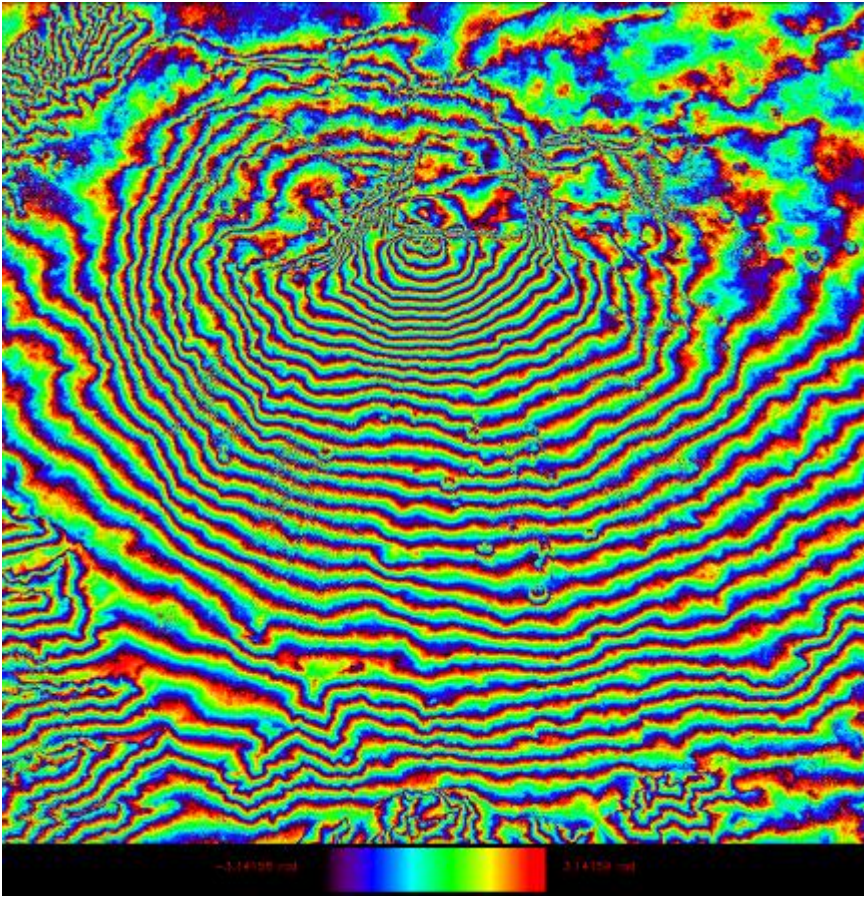


Topographic phase



RawMaterials

Connecting matters



Baseline doubling



This activity has received funding from the European Institute of Innovation and Technology (EIT), a body of the European Union, under the Horizon 2020, the EU Framework Programme for Research and Innovation

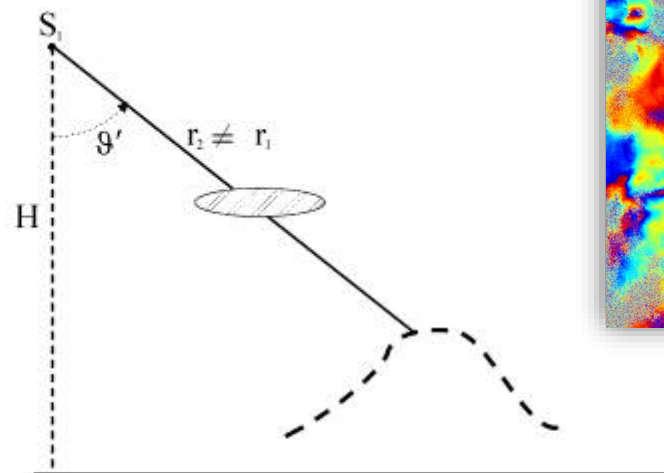
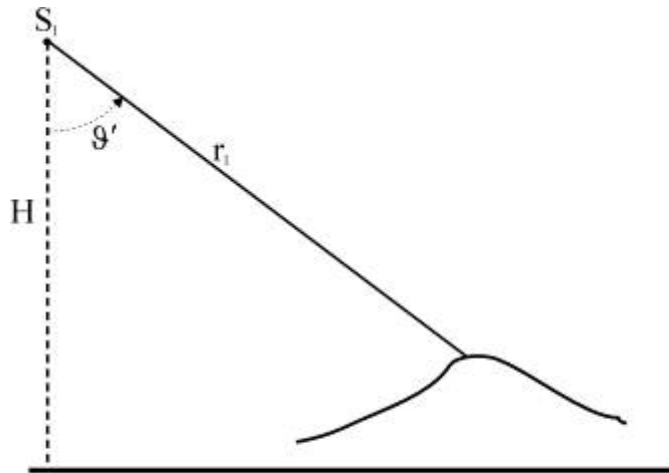
Supported by:  RawMaterials
Connecting matters

Atmospheric phase

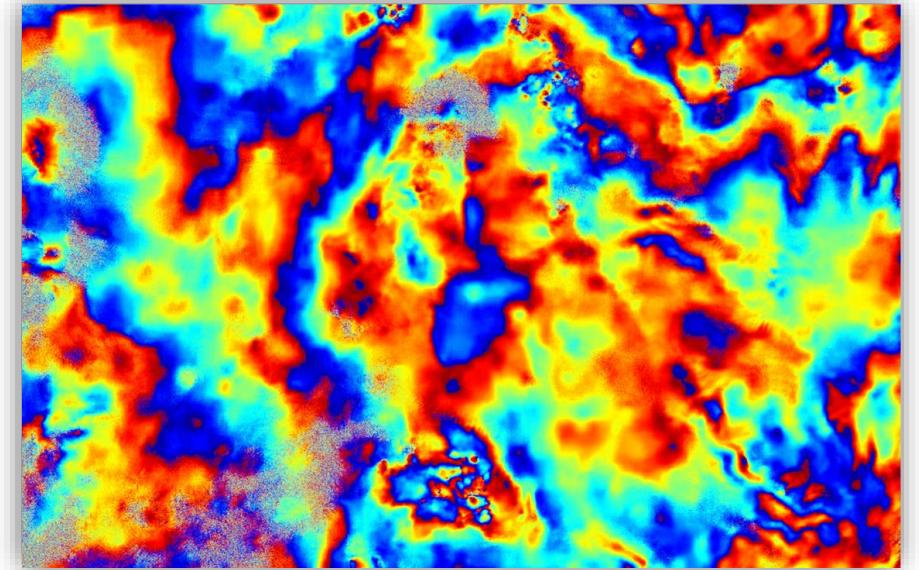
$$\phi_{atm} = \frac{4\pi}{\lambda} \Delta l \implies$$

$$\Delta l = \int_0^L (n - 1) dl$$

$$n - 1 = \frac{77.6}{T} \left(P_t + 4810 \frac{P_w}{T} \right) 10^{-6}$$



Change in the propagation path
due to atmospheric turbulence, no deformation



Atmospheric phase

- The phase due to atmospheric artifacts does not depend on the baseline
- The sensitivity of the phase to the atmosphere is related to the wavelength
- Longer wavelengths are less sensitive to atmospheric distortions
- A propagation delay of 2 cm would result in an additional phase of an almost full fringe at C-band but only of 1/6th of a fringe at L-band



Complex coherence

... or Phase Coherence

The degree of correlation between two SAR images is measured by the coherence parameter.

The amplitude is the degree of coherence, the phase is the interferometric phase.

$$\gamma = \frac{E(s_1 s_2^*)}{\sqrt{E(s_1 s_1^*) E(s_2 s_2^*)}}$$

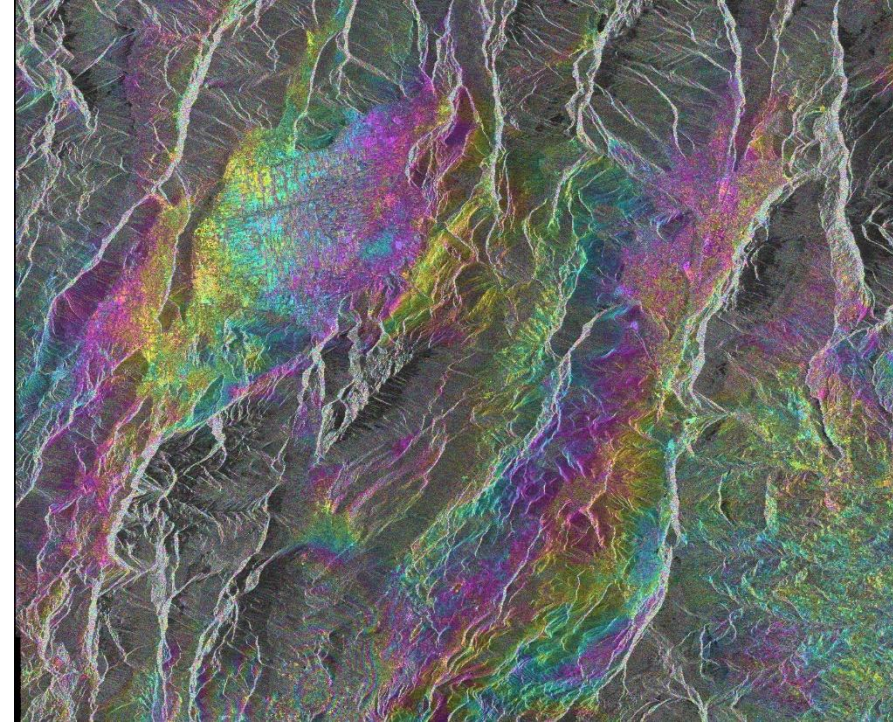
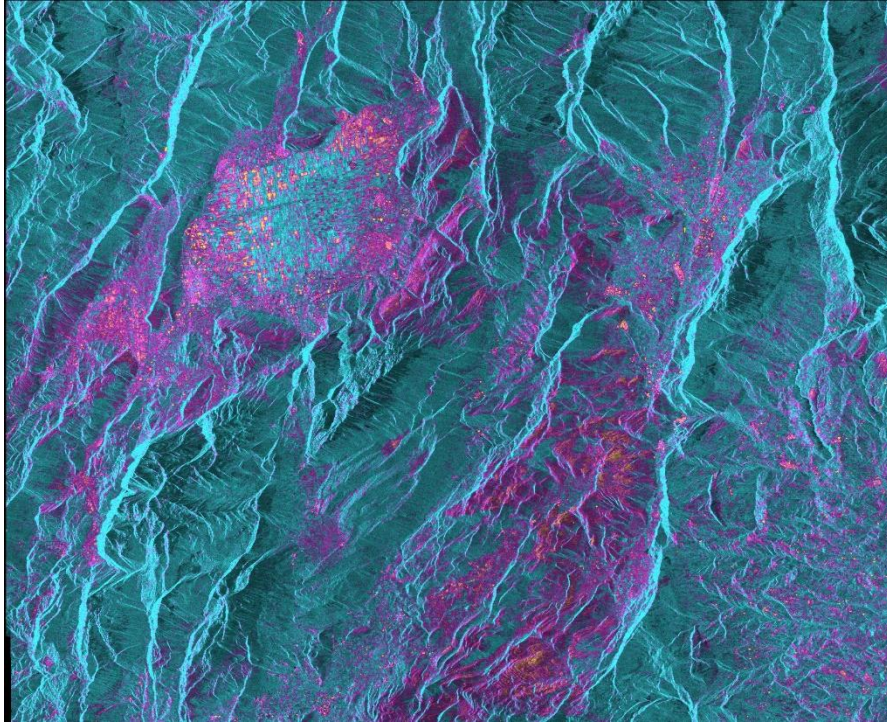


Complex coherence



RawMaterials

Coherence



Interferometric phase

- When the coherence is close to zero, total decorrelation has occurred.
- Coherence close to 1 indicates a very stable and strong scattering object.
- Coherence is a measure of the phase noise or fringe visibility



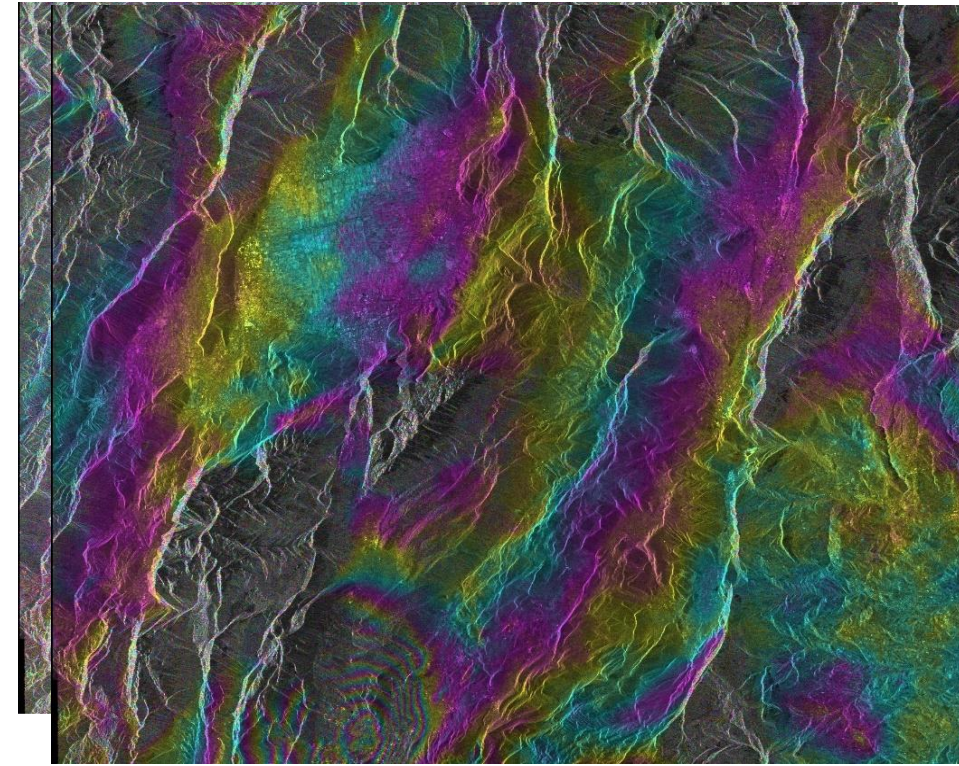
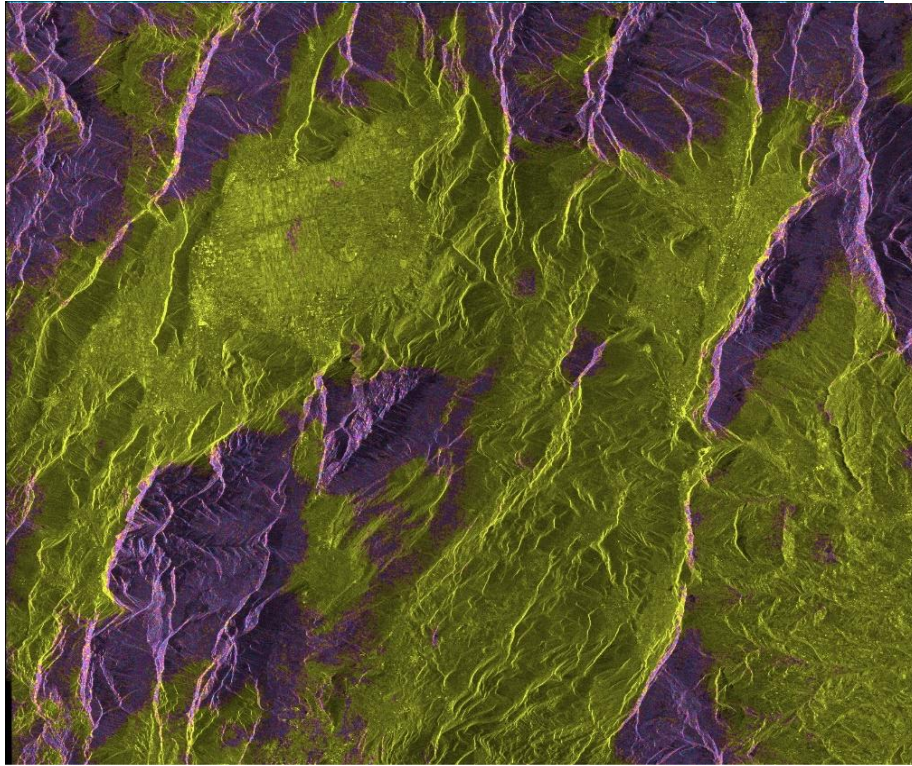
This activity has received funding from the European Institute of Innovation and Technology (EIT), a body of the European Union, under the Horizon 2020, the EU Framework Programme for Research and Innovation

Supported by:  RawMaterials
Connecting matters

Complex coherence filtering

...and reduce phase noise to improve fringe visibility

Coherence



Interferometric phase



Complex coherence

$$|\gamma| = \cancel{|\gamma|_{processor}} \cdot \cancel{|\gamma|_{noise}} \cdot \cancel{|\gamma|_{azimuth}} \cdot |\gamma|_{spatial} \cdot |\gamma|_{temporal}$$

In the end the coherence is related to the

correlation in space $|\gamma|_{spatial}$

correlation in time $|\gamma|_{temporal}$

- The spatial coherence can be filtered out. A part remains if we have a volume (forest, snow, city,...). This is called volume decorrelation and increases with the spatial baseline.
- The temporal coherence can NOT be filtered out, it is a property of the image. This is also referred to as temporal decorrelation term and depends on the stability of the objects between the two acquisitions.



Complex coherence

Geometric decorrelation: it relies on the sight angle differences of the two SAR scenes of the interferogram. The critical value of the baseline at which complete decorrelation occurs is given by:

$$B_c = \frac{\lambda R}{2r_d \cos^2 \theta}$$

- For Sentinel-1 (C-band) the critical baseline is about 1100 m (R=850 km, $\theta=23^\circ$, $\lambda=5.6$ cm).
- For ALOS-PALSAR (L-band) the critical baseline is about 4 km (R=730 km, $\theta=35^\circ$, $\lambda=23$ cm).



Complex coherence

The radar pulse samples a small bandwidth of the spatial reflectivity spectrum of the surface. Because the second antenna sees the scene under a slightly different angle, it records a different part of the spectrum shifted by an amount Δf .



$$\Delta f = -\frac{cB_{\perp}}{R\lambda \tan \theta}$$

If images are processed like this, they automatically lose part of the correlation they have (=spatial decorrelation). Spectral shift filtering removes the effect of spatial decorrelation for level surfaces. There is a proportional loss of range resolution.

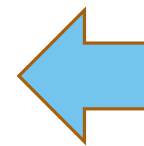
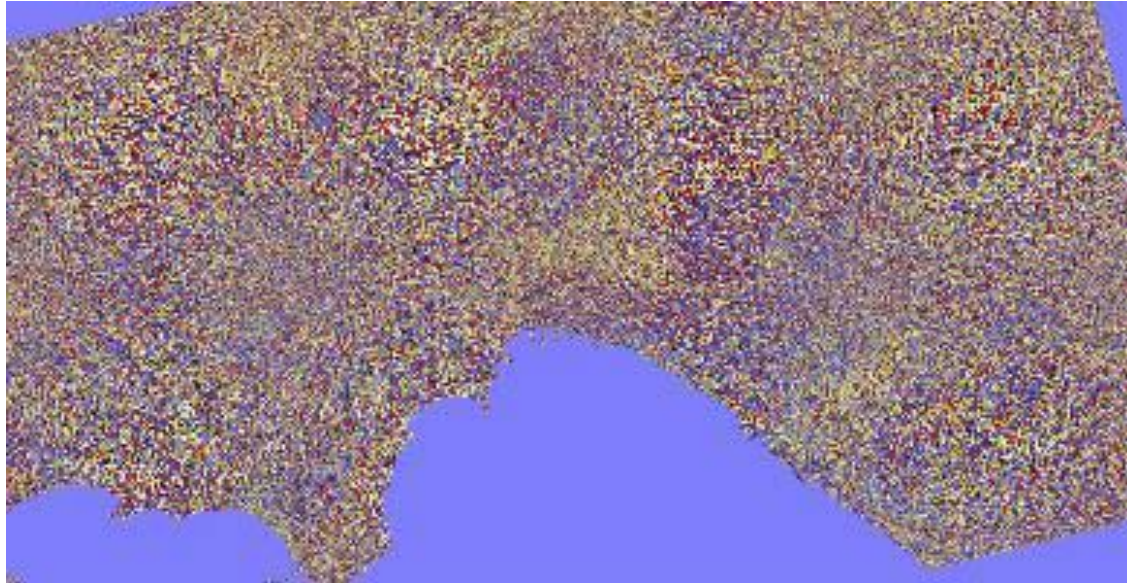


Complex coherence

- In the repeat-pass configuration the scatterers may move (e.g. water surfaces and tree canopies) or their dielectric properties may change (e.g. snow, wet soils) between observations.
- The two SAR images are only partially correlated because of the temporal interval between the acquisitions.
- In general it is likely that the longer the time interval between acquisitions, the stronger the temporal decorrelation.
- Taking into account that typically temporally unstable scatterers have dimensions of the order of a few centimeters or less (e.g. leaves, grass, snow grains etc.), temporal decorrelation is more pronounced at shorter wavelengths, e.g. at X- and C-band.

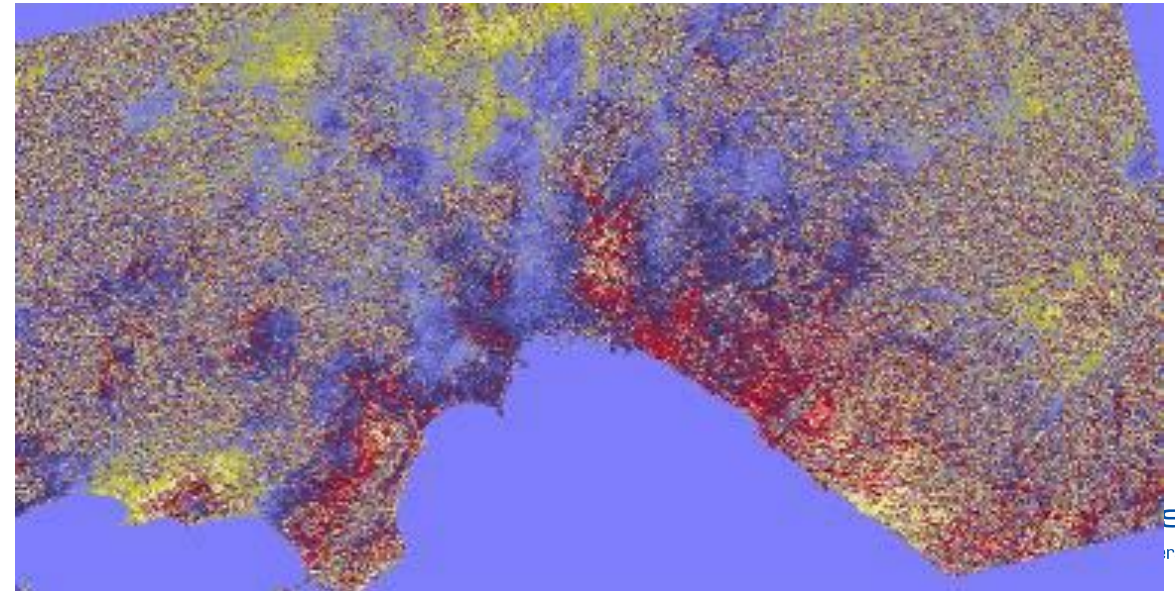
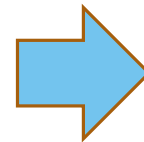


Spatial decorrelation effects



06/02/1997-22/05/1997
Baseline ort. = 330 m

22/05/1997-18/12/1997
Baseline ort. = 40 m

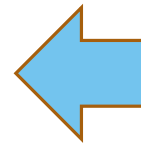
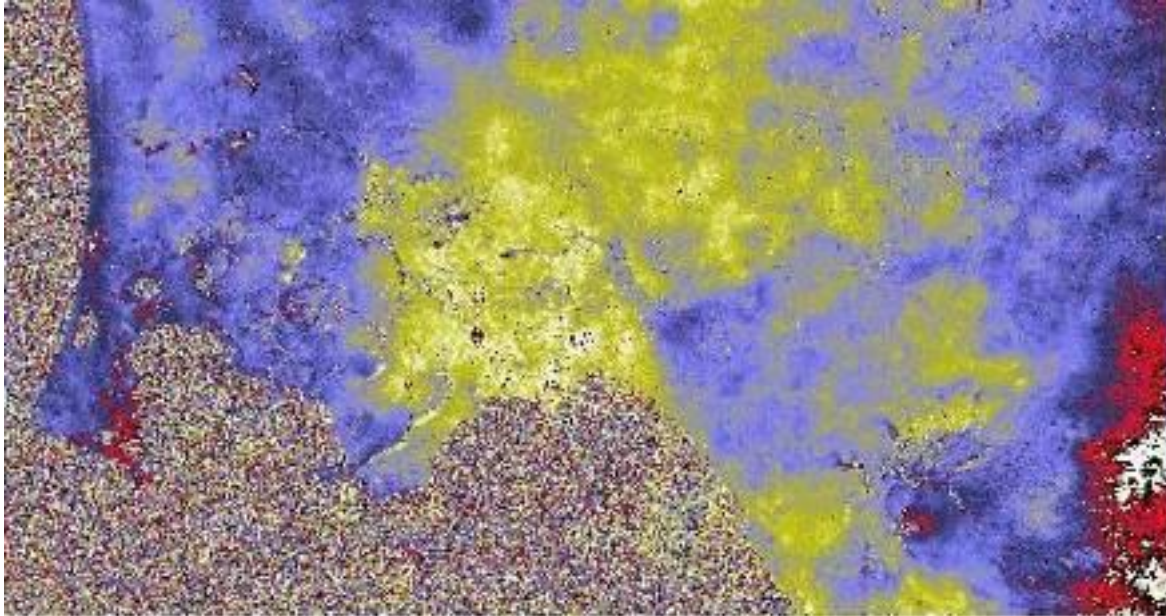


Temporal decorrelation effects



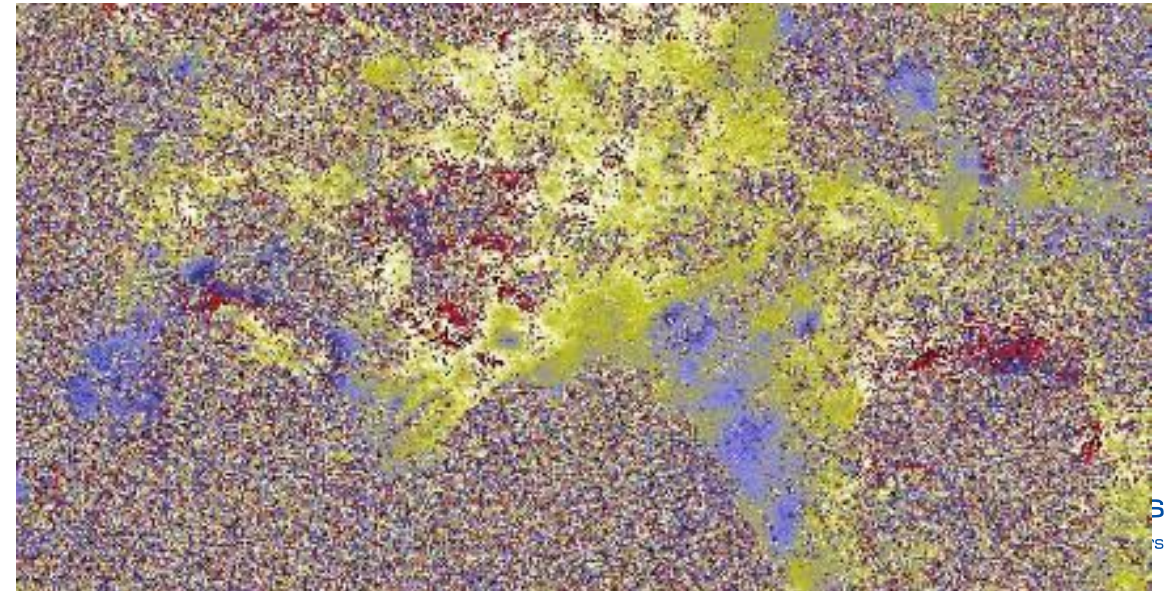
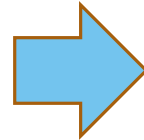
RawMaterials

Connecting matters



07/05/1996-08/05/1996
Baseline temp. = 1 day

02/06/1999-06/02/2002
Baseline temp. = 980 days
Baseline ort. = 3 m



This activity has received funding from the European Institute of Innovation and Technology (EIT), a body of the European Union, under the Horizon 2020, the EU Framework Programme for Research and Innovation

Decorrelation & wavelength

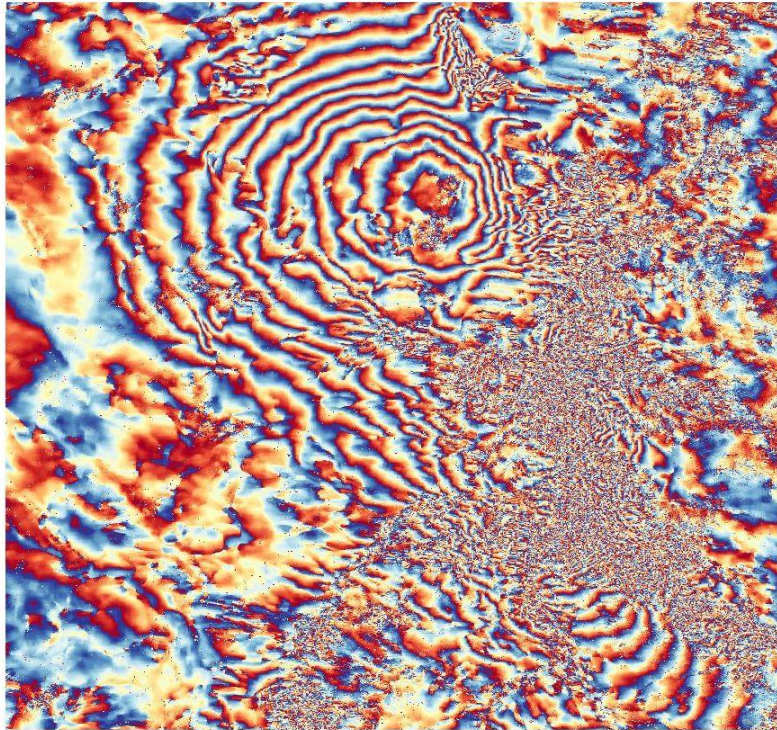


RawMaterials

Connecting matters

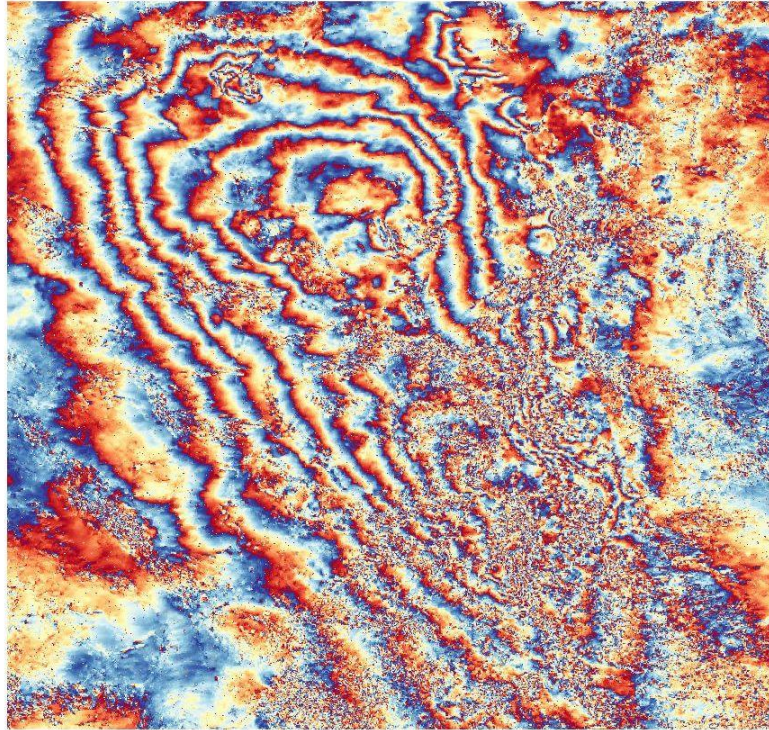
X band

$\lambda=3.1\text{cm}$ $\Delta t=8$ days



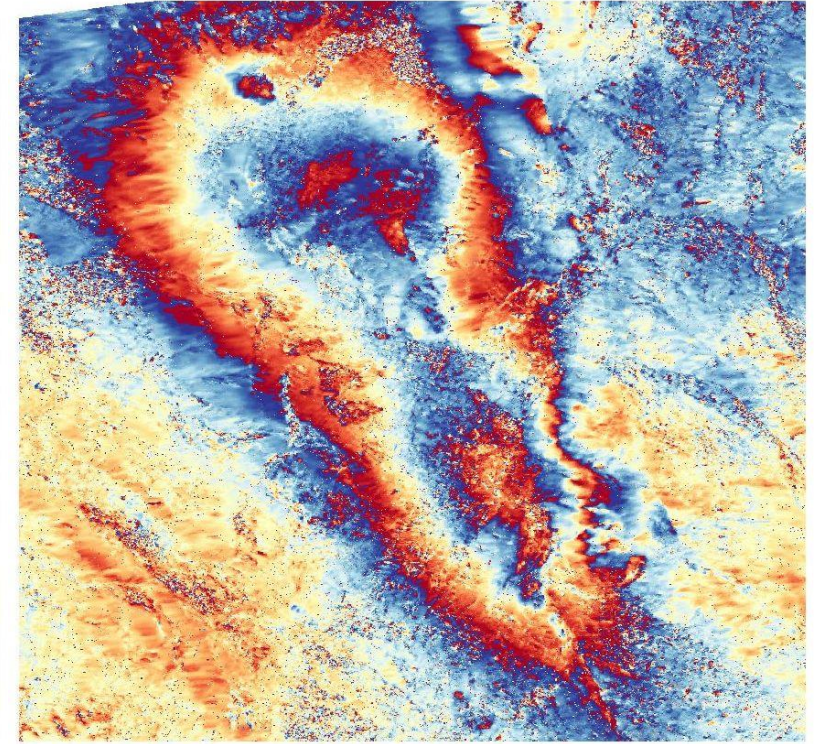
C band

$\lambda=5.6\text{cm}$ $\Delta t=6$ days



L band

$\lambda=23\text{cm}$ $\Delta t=8$ days



This activity has received funding from the European Institute of Innovation and Technology (EIT), a body of the European Union, under the Horizon 2020, the EU Framework Programme for Research and Innovation

Supported by:  RawMaterials
Connecting matters

Phase Coherence and accuracy



RawMaterials

Connecting matters

- Phase Coherence can also be used to estimate the expected phase noise, hence the expected accuracy of the interferometric product:

$$\sigma_{\varphi} = \frac{\sqrt{1 - \gamma^2}}{\gamma \sqrt{2N}}$$

where:

g = coherence value

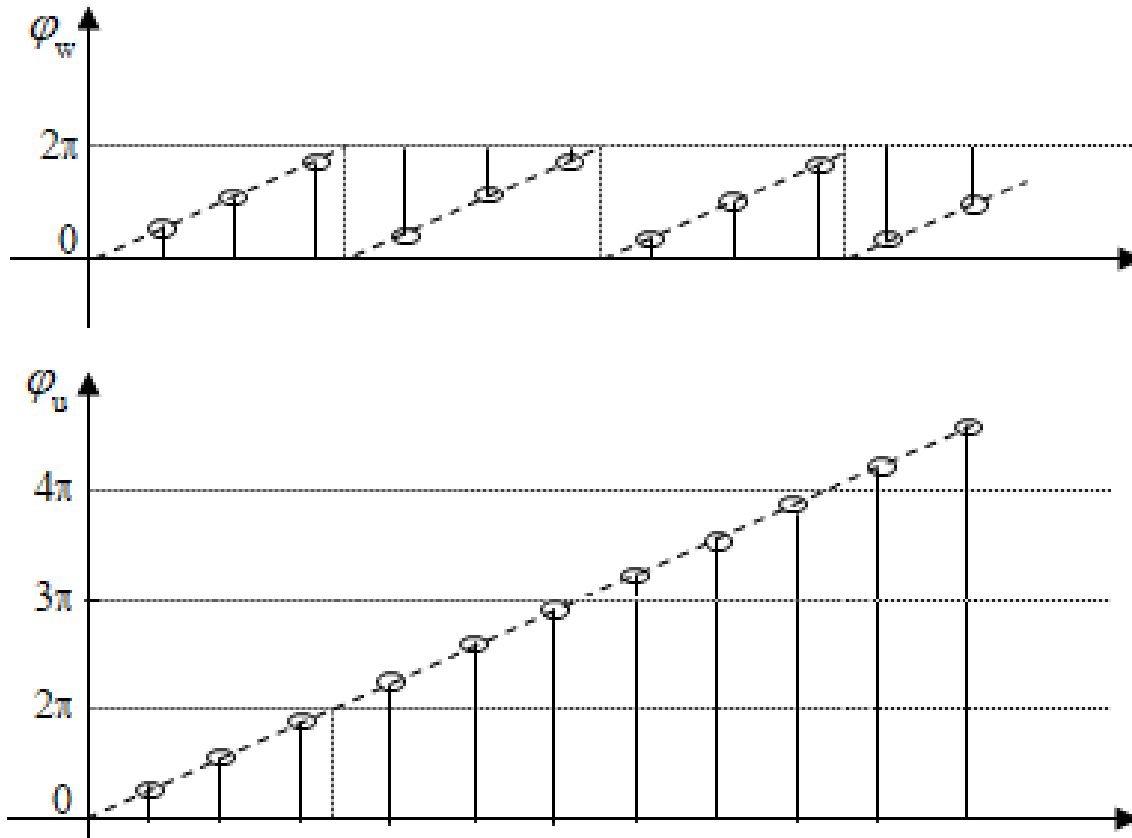
N = look number



This activity has received funding from the European Institute of Innovation and Technology (EIT), a body of the European Union, under the Horizon 2020, the EU Framework Programme for Research and Innovation

Supported by:  RawMaterials
Connecting matters

Phase ambiguity & Phase unwrapping



The interferometric phase is modulus 2π

A phase unwrapping method can be then applied to calculate the exact phase value



Phase ambiguity

The interferometric phase component is known excepting for $2N\pi$:

$$\varphi_{\text{int}} = \varphi_f + \varphi_{\text{topo}} + \varphi_{\text{displ}} + \varphi_{\text{atm}} + \varphi_{\text{err}} + 2N\pi$$

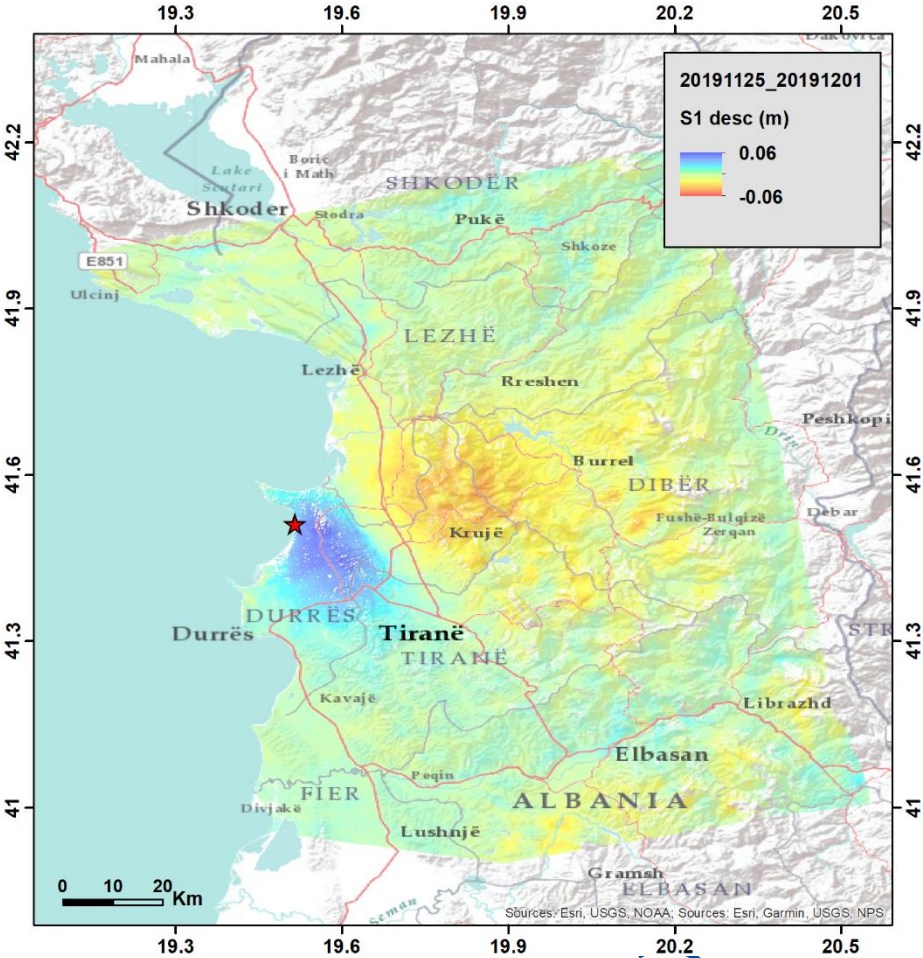
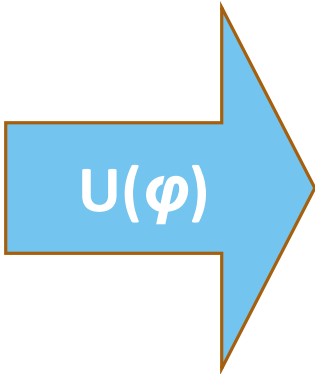
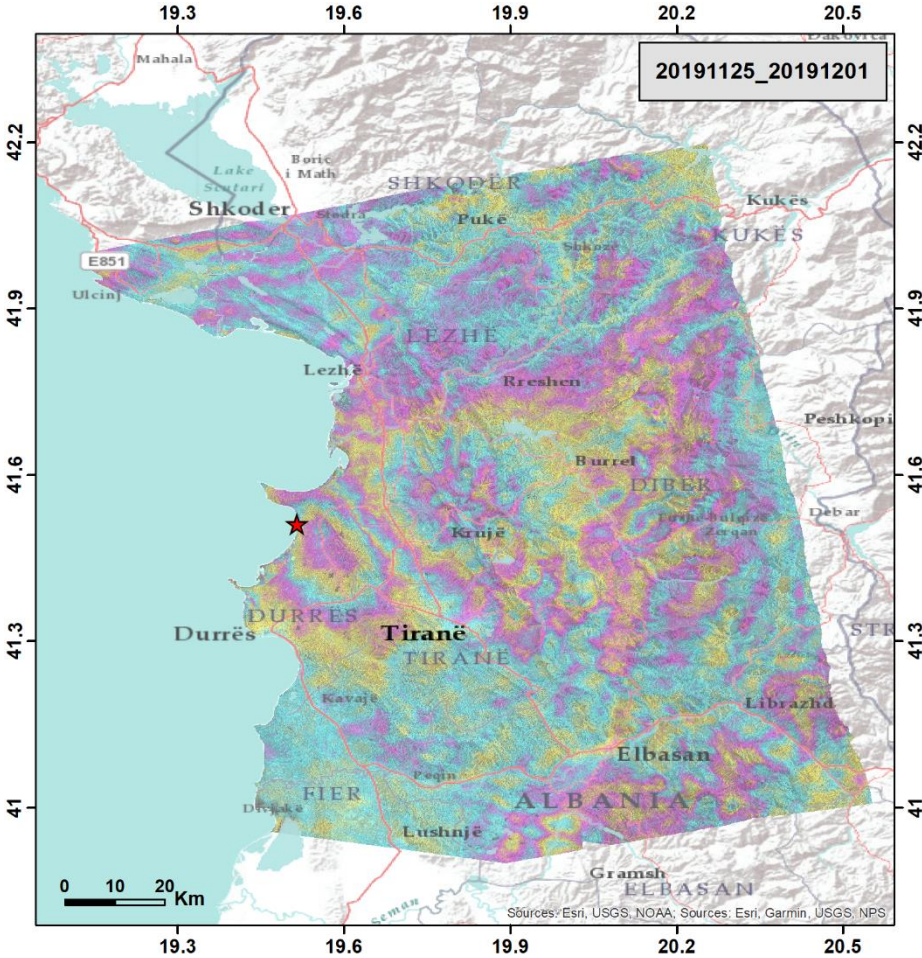
Phase unwrapping algorithms can be applied to retrieve f from the “wrapped phase” :

minimum cost flow (MCF) techniques is one of the most used among others such as Branch Cut and triangular irregular network (TIN)

$$\varphi_m = \langle \varphi \rangle$$
$$] - \pi, \pi]$$



From Phase to Deformation



This activity has received funding from the European Institute of Innovation and Technology (EIT), a body of the European Union, under the Horizon 2020, the EU Framework Programme for Research and Innovation

Differential SAR Interferometry (DInSAR)

- Objective of DInSAR: Separation of φ_{topo} from total phase to determine φ_{displ}
- 2-pass: Simulate φ_{topo} based on existing DEM. Phase unwrapping not required for the simulated interferogram. High accuracy of DEM required.
- 3- and 4-pass: Derive φ_{topo} from independent interferogram, no existing DEM is required but phase unwrapping required.



Differential SAR Interferometry (DInSAR)



- Differential SAR Interferometry (DInSAR) is an InSAR technique addressed to measure the Earth surface displacements with centimetric accuracy.
- DInSAR is used in seismology, for instance, when an earthquake takes place. Two SAR images, one pre-seismic, one post-seismic, are acquired.
- The interferometric phase is computed. Using a DEM the topographic phase is cancelled.
- The residual phase contains also the eventual surface deformation effect (differential interferogram).
- Each differential fringe corresponds to a full phase cycle (2π) and represents a sensor-to-target distance change (LOS change) of $\lambda/2$.
- For C-Band sensors it is about 2.8 cm.



This activity has received funding from the European Institute of Innovation and Technology (EIT), a body of the European Union, under the Horizon 2020, the EU Framework Programme for Research and Innovation

Differential SAR Interferometry (DInSAR)

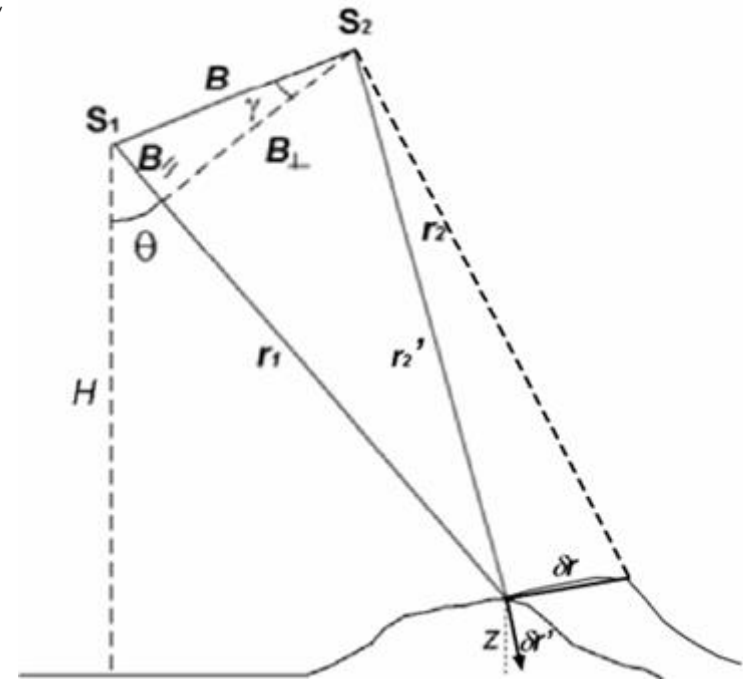
Be S_1 and S_2 two SAR satellites. The interferometric phase is:

$$\varphi_{\text{int}} = \cancel{\varphi_f} + \cancel{\varphi_{\text{topo}}} + \varphi_{\text{displ}} + \varphi_{\text{atm}} + \varphi_{\text{err}} + 2N\pi$$

$$\Delta\varphi = \frac{4\pi}{\lambda}(r_1 - r_2) = \frac{4\pi}{\lambda}(r_1 - r_2) + \frac{4\pi}{\lambda}(r_2' - r_2) = \varphi_{\text{topo}} + \varphi_{\text{displ}}$$

$$\varphi_{\text{displ}} = \frac{4\pi}{\lambda} \delta' r$$

The residual phase contains, besides atmosphere and noise, the displacement projected onto the LOS.



DInSAR displacement accuracy

$$\phi_d = \frac{4\pi}{\lambda} \Delta r \quad \longrightarrow \quad \Delta r = \frac{\lambda}{4\pi} \phi_d \quad \longrightarrow \quad \sigma_{\Delta r} = \frac{\lambda}{4\pi} \sigma_{\phi_d}$$

By considering a standard deviation on phase:

For C-Band:

$$\lambda = 5.6 \text{ cm}$$

$$\sigma_{\Delta r} = 0.25 \text{ cm}$$

$$\sigma_{\phi_t} = \frac{\pi}{6}$$

$$\left[\text{with } b_{\perp} = 0 \text{ m} \right]$$



In conclusion

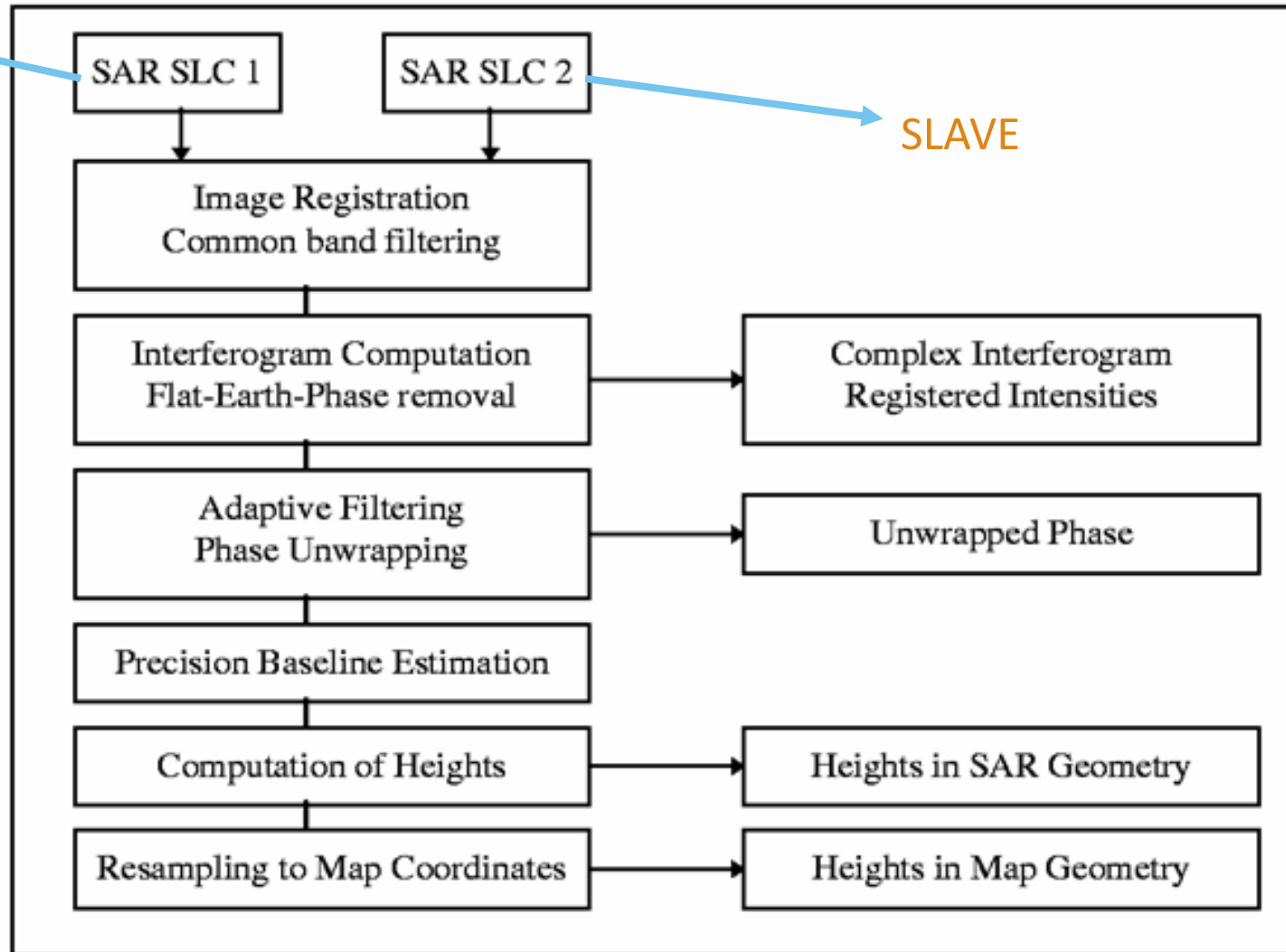
$$\varphi_{\text{int}} = \varphi_f + \varphi_{\text{topo}} + \varphi_{\text{displ}} + \varphi_{\text{atm}} + \varphi_{\text{err}} + 2N\pi$$

$$\Delta\varphi \cong \frac{4\pi}{\lambda} B \cdot \sin \gamma + \frac{4\pi}{\lambda} B_{\perp} \cdot \frac{z}{r_1 \sin \vartheta} + \frac{4\pi}{\lambda} \delta' r + \frac{4\pi}{\lambda} \Delta L + \Delta\varphi_{\text{err}} + 2N\pi$$



Interferogram generation

MASTER

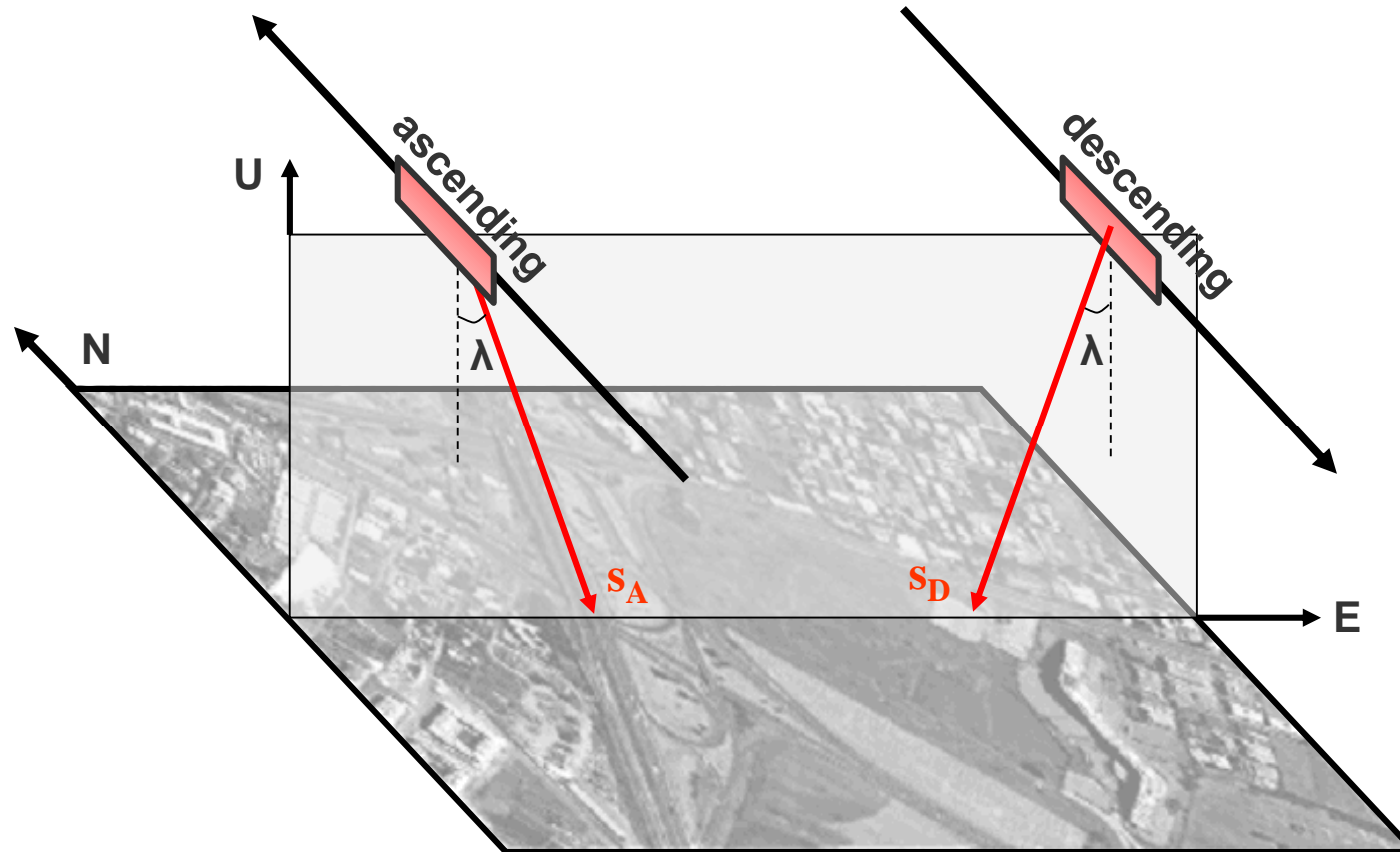


Descending vs ascending interferograms



RawMaterials

Connecting matters



This activity has received funding from the European Institute of Innovation and Technology (EIT), a body of the European Union, under the Horizon 2020, the EU Framework Programme for Research and Innovation

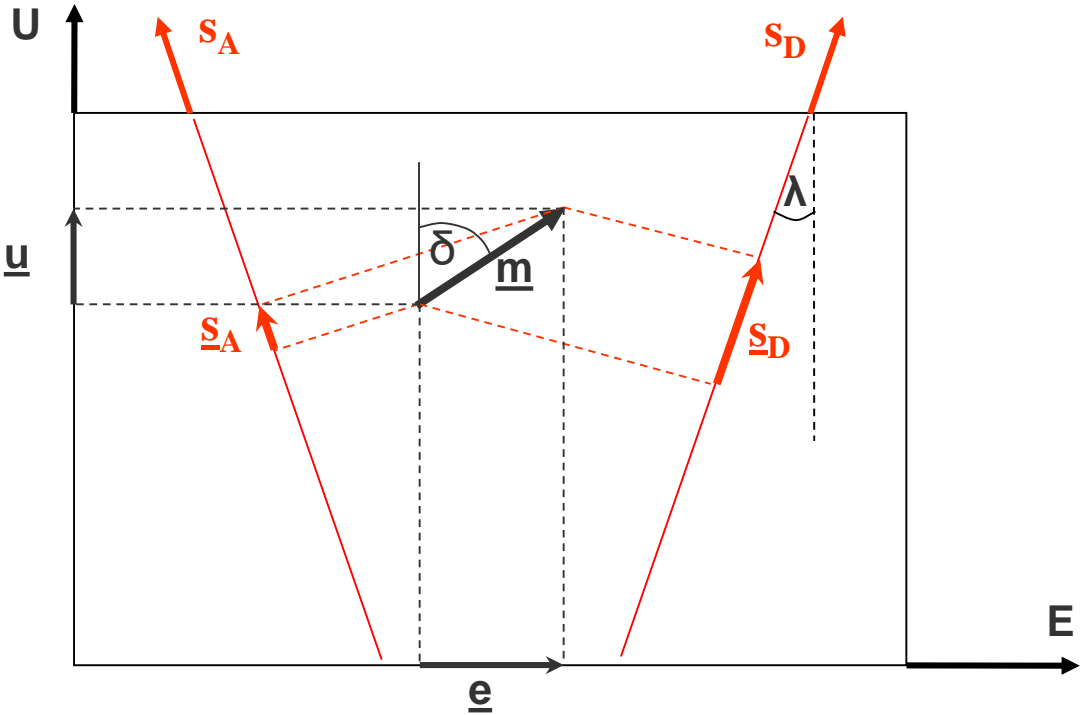
Supported by:  RawMaterials
Connecting matters

Displacement in Up and East direction



RawMaterials

Connecting matters



e and u components from slant range ascending and descending *a* and *d*

$$EAST \approx \frac{d - a}{2 * \sin \theta \cos \alpha}$$

$$UP \approx \frac{d + a}{2 * \cos \theta}$$

look angle (λ) = 23°

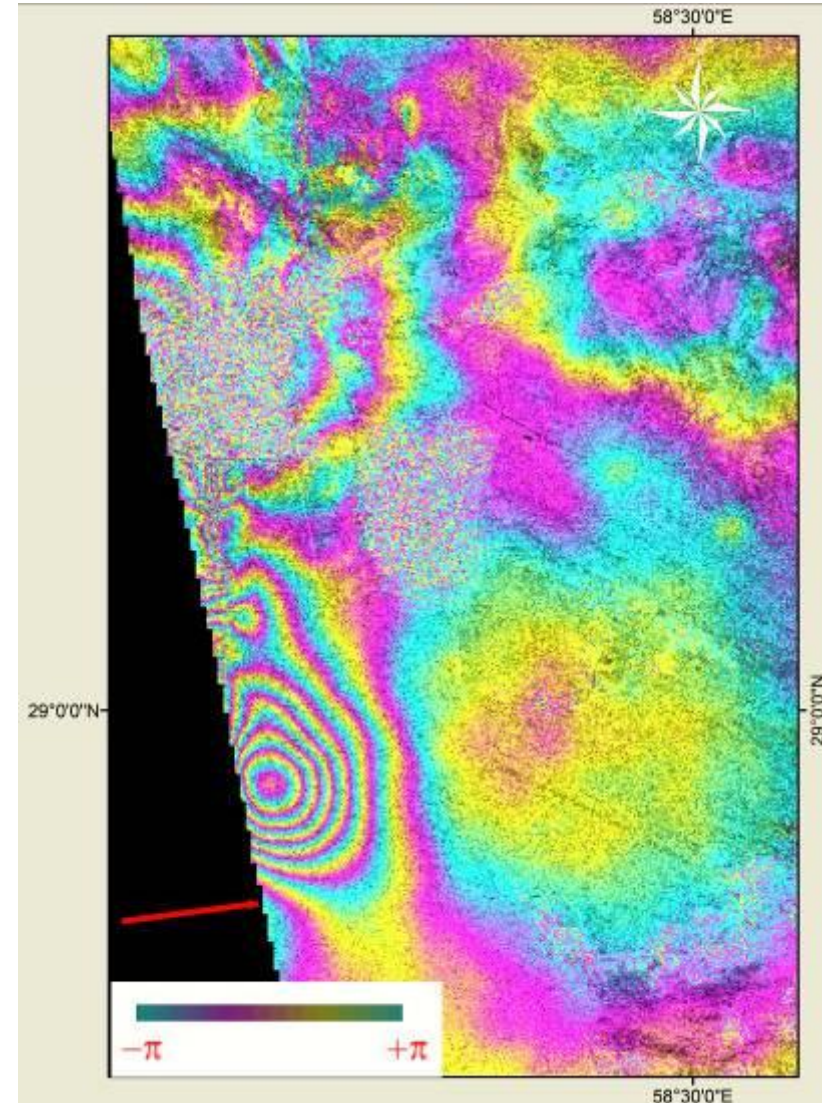
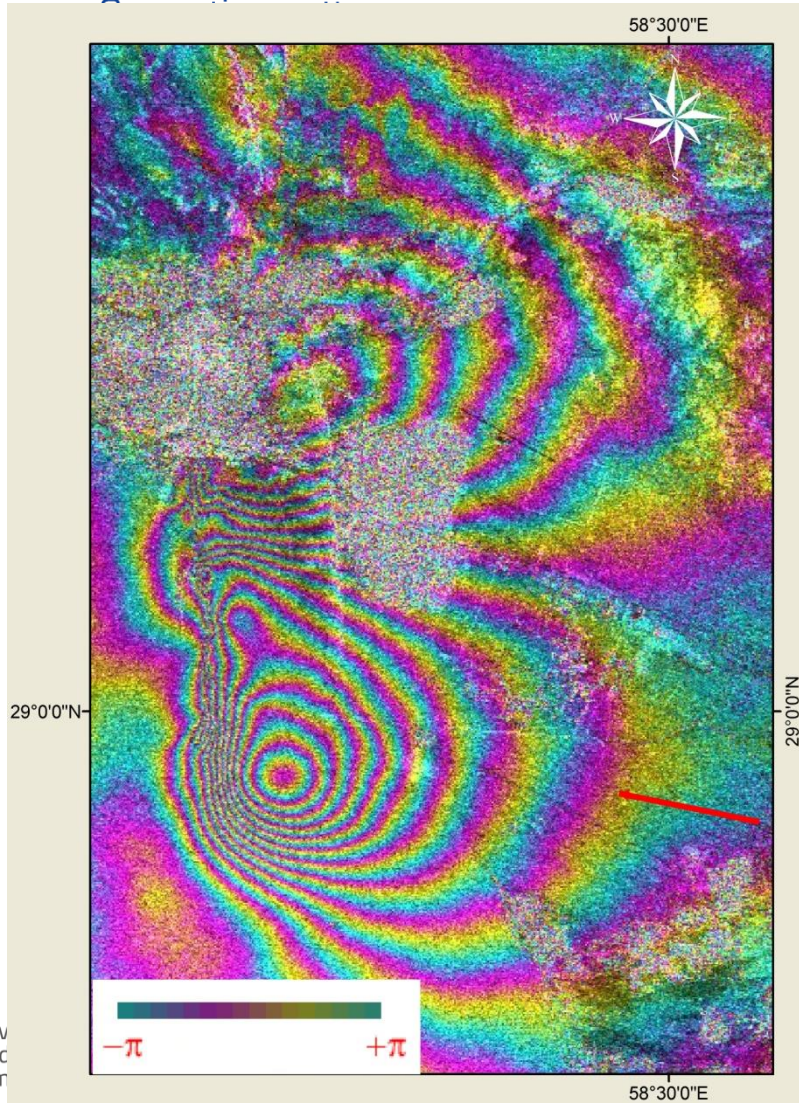
$$\delta = \lambda + \arctan\left(\frac{1}{\tan 2\lambda} - \frac{s_A}{s_D \sin 2\lambda}\right)$$

Conversely:
$$\begin{bmatrix} \cos(\theta) & -\sin(\theta) \cos(\alpha) & \sin(\theta) \sin(\alpha) \end{bmatrix} \begin{bmatrix} D_U \\ D_E \\ D_N \end{bmatrix} = \Delta R$$

Descending vs ascending interferograms



RawMaterials



This activity has received funding from the European Union's Horizon Europe Research and Innovation Programme under grant agreement No 101019719.



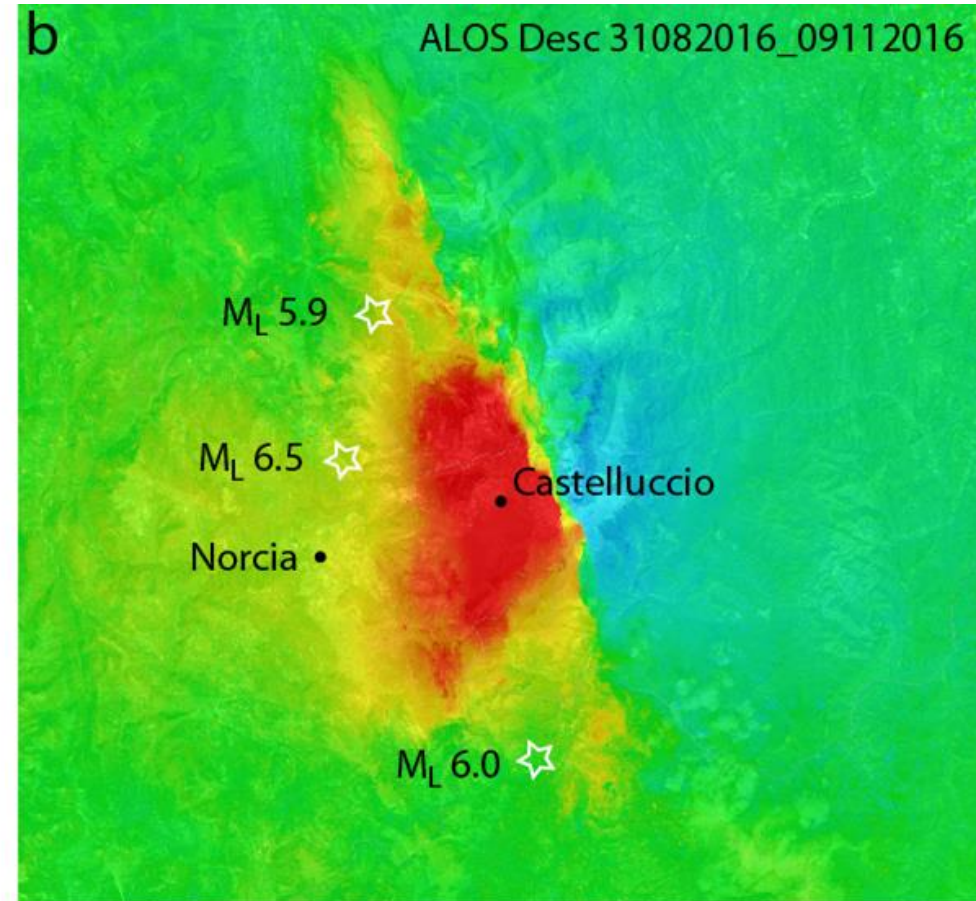
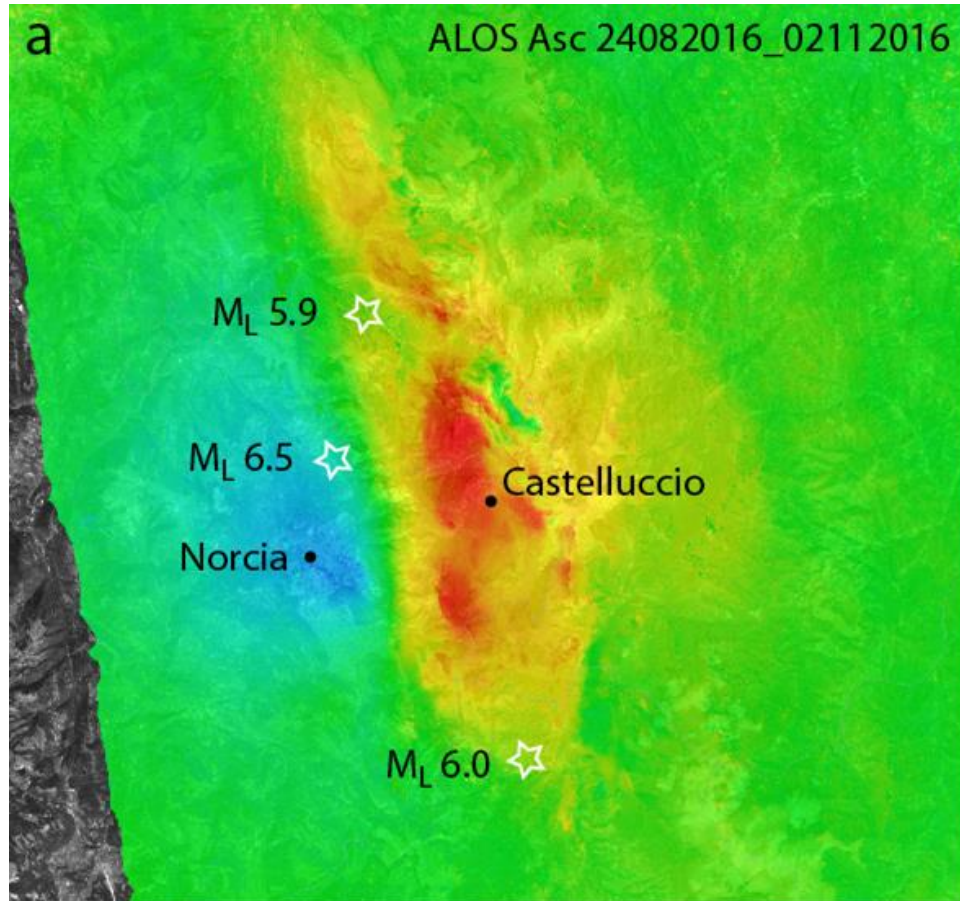
RawMaterials
Connecting matters

From Ascending and Descending interferograms....



RawMaterials

Connecting matters



LOS Displacement [cm]



This act
Techno
Framework Programmé for Research and Innovation



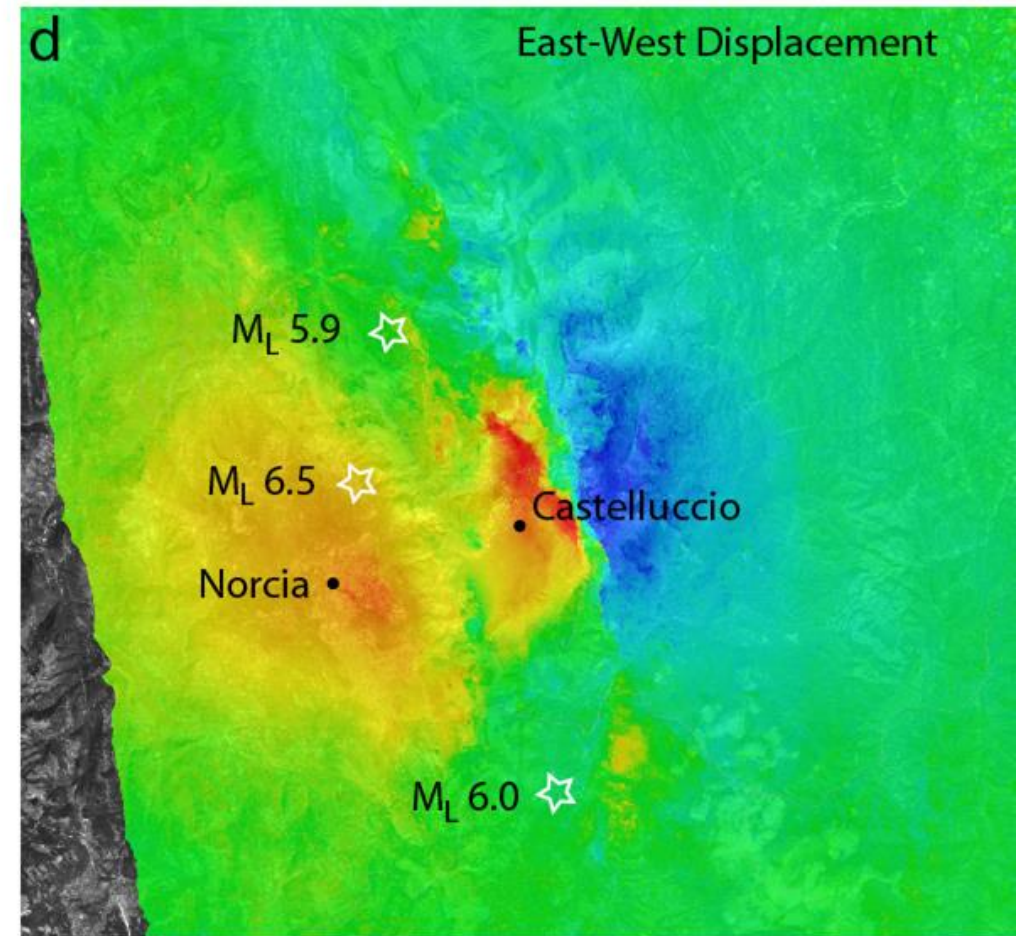
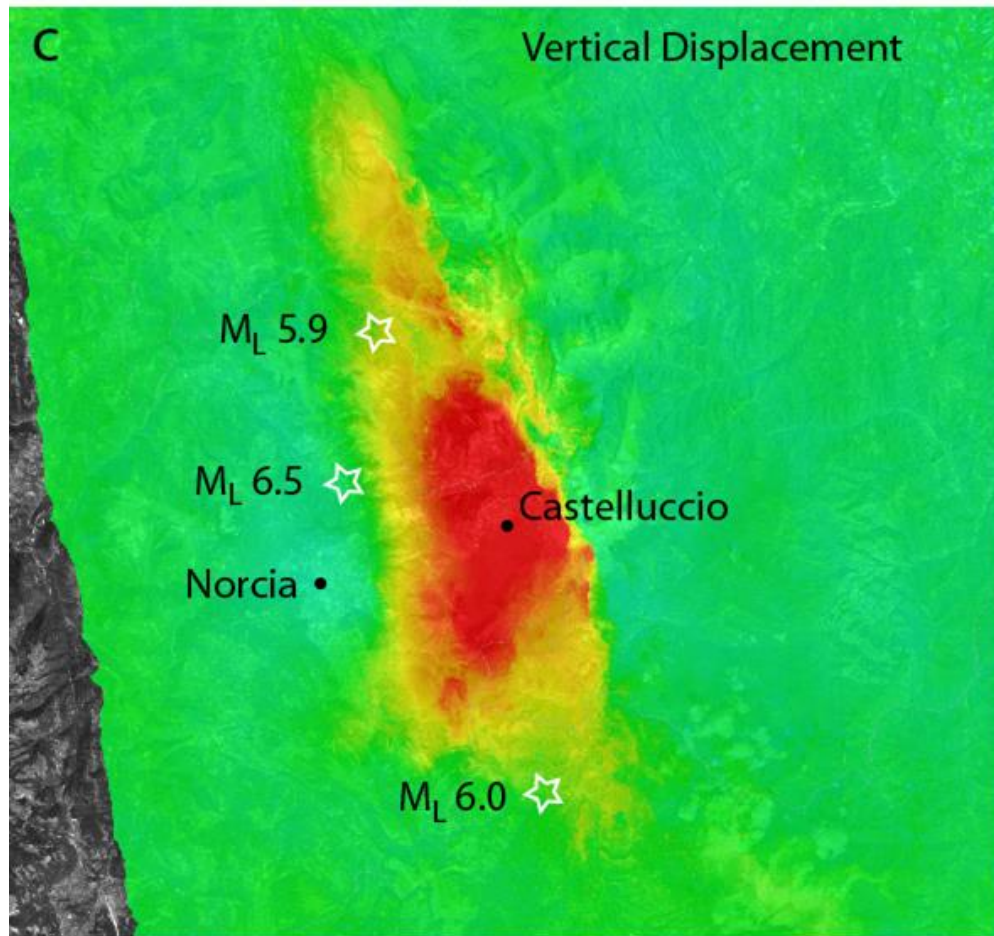
Materials
Connecting matters

To Displacement in Up and East directions



RawMaterials

Connecting matters



This ac
Techno
Frame



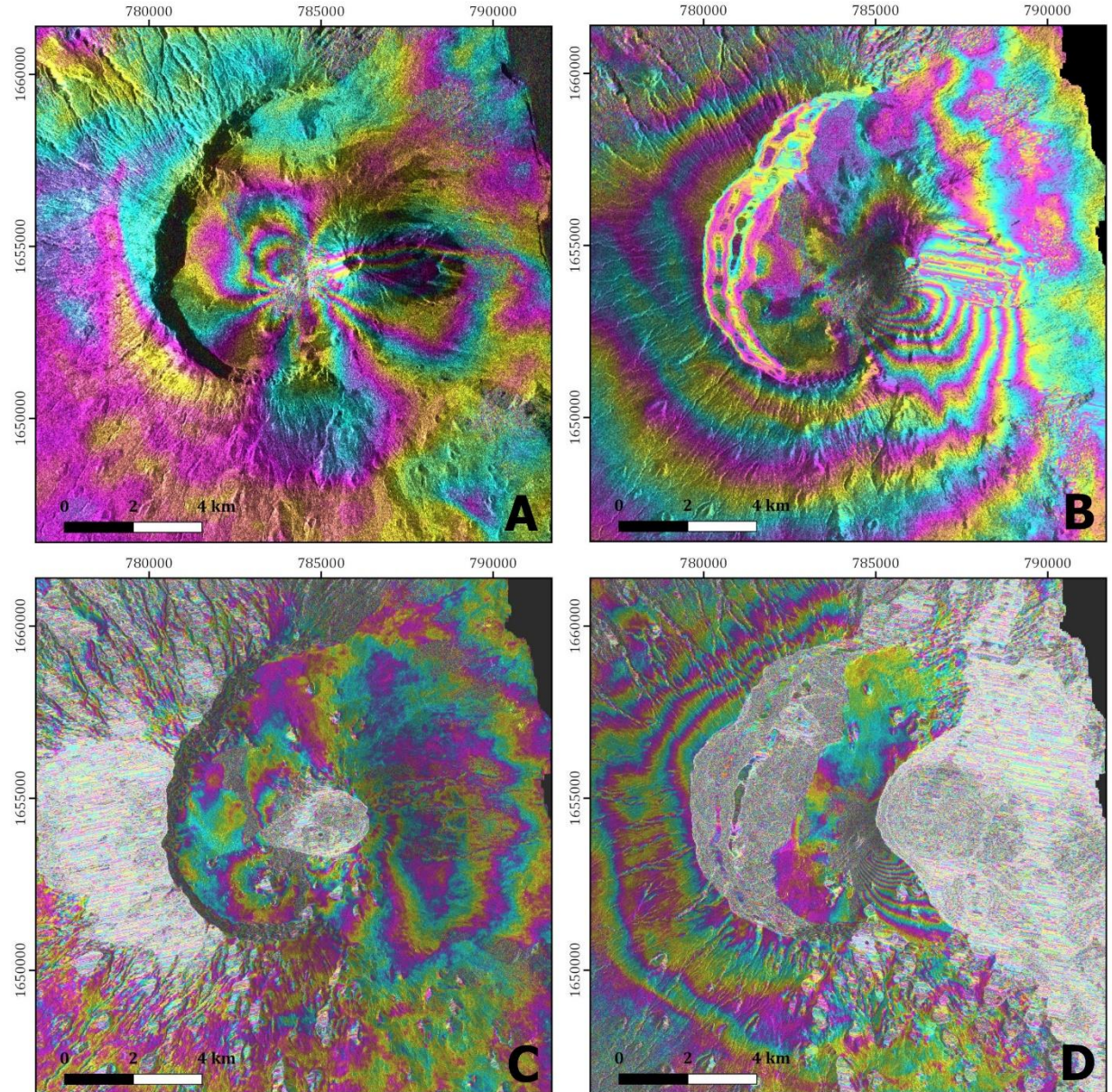
erials
cting matters



RawMaterials
Connecting matters

Sentinel & COSMO- SkyMed InSAR

Wrapped interferograms

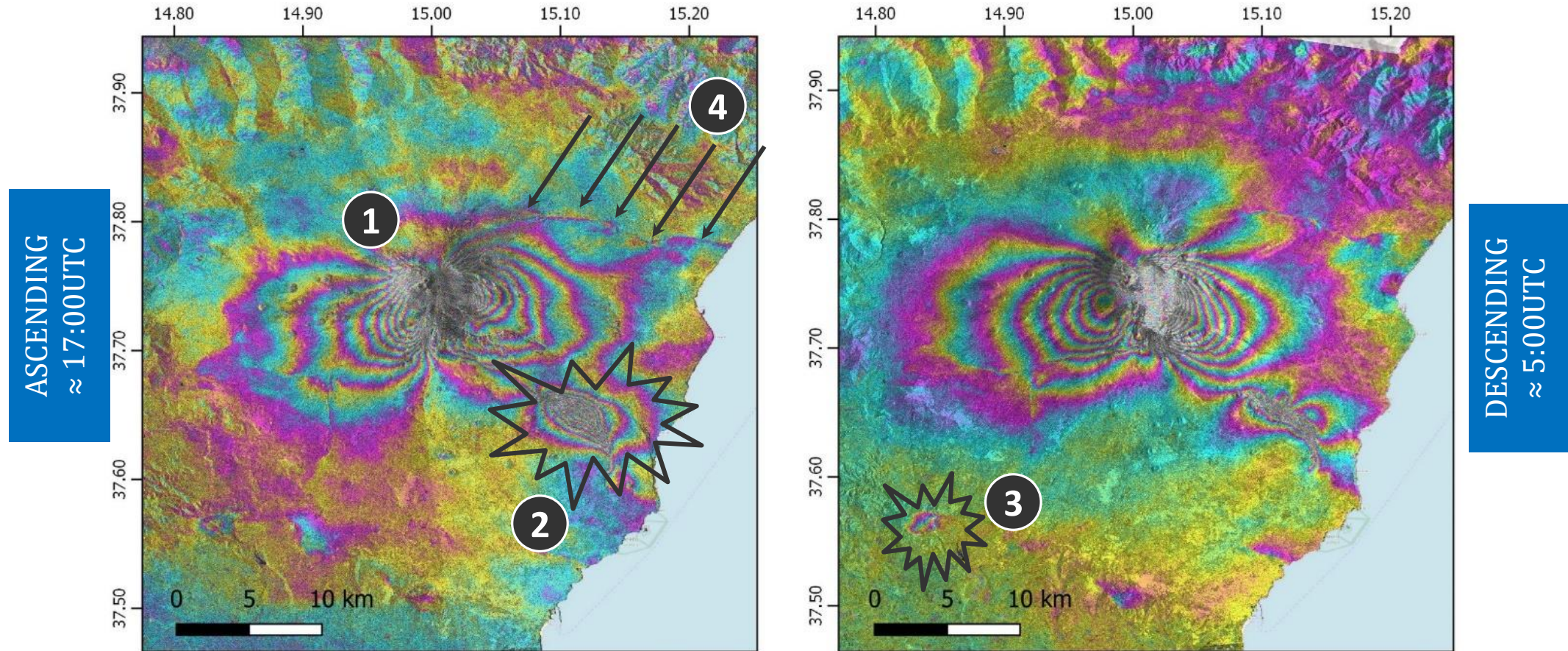


This activity has received funding from the European Institute of Innovation and Technology (EIT), a body of the European Union, under the Horizon 2020, the EU Framework Programme for Research and Innovation

Full ground deformation map

What we have seen in a single InSAR shot...

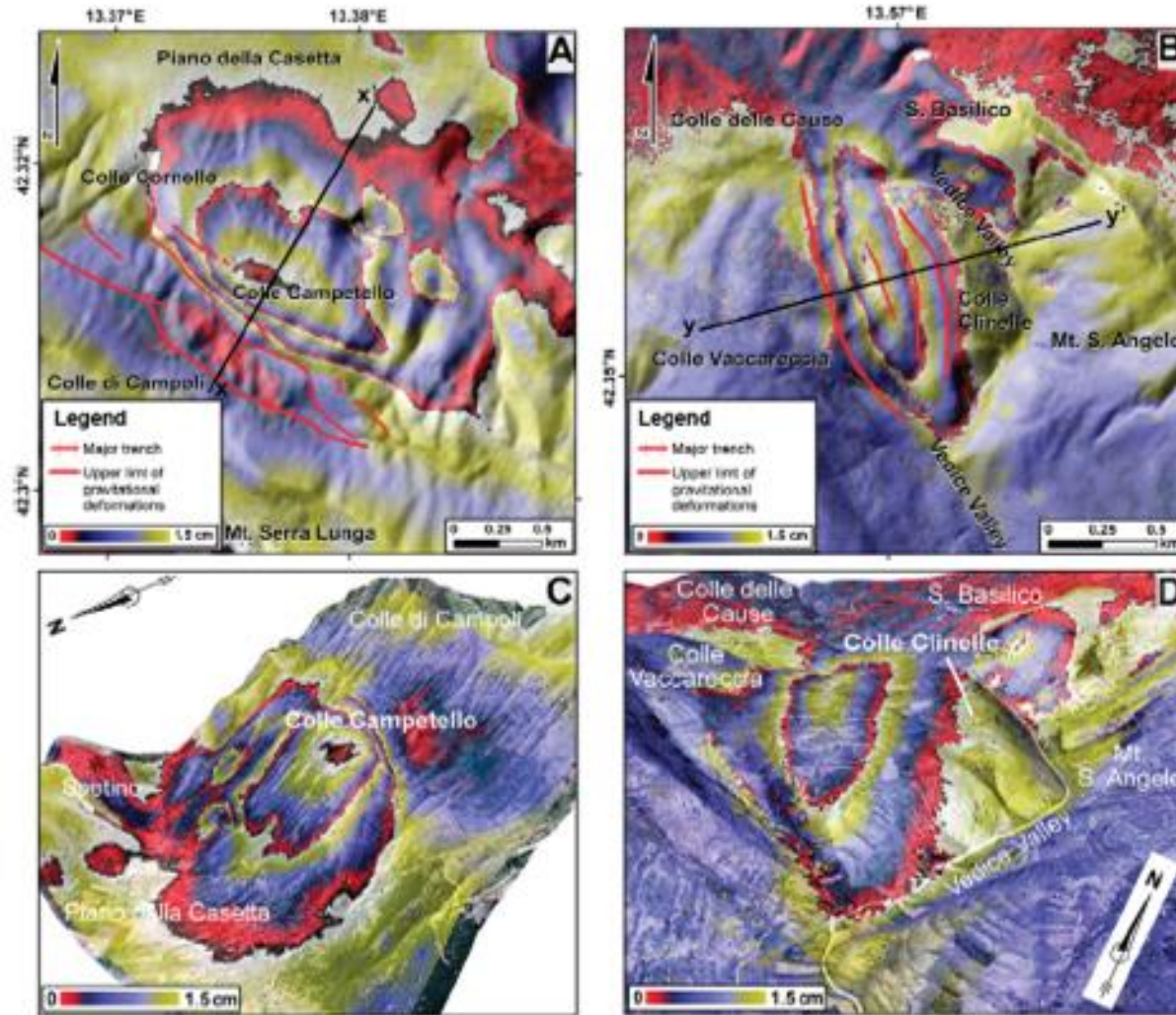
22 December 2018 & 28 December 2018, only 6 days separation



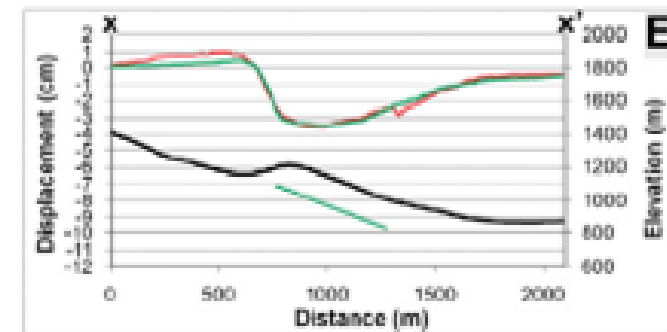
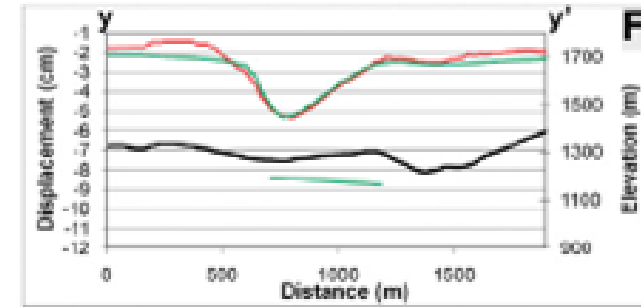
≈2.7 cm per colour cycle



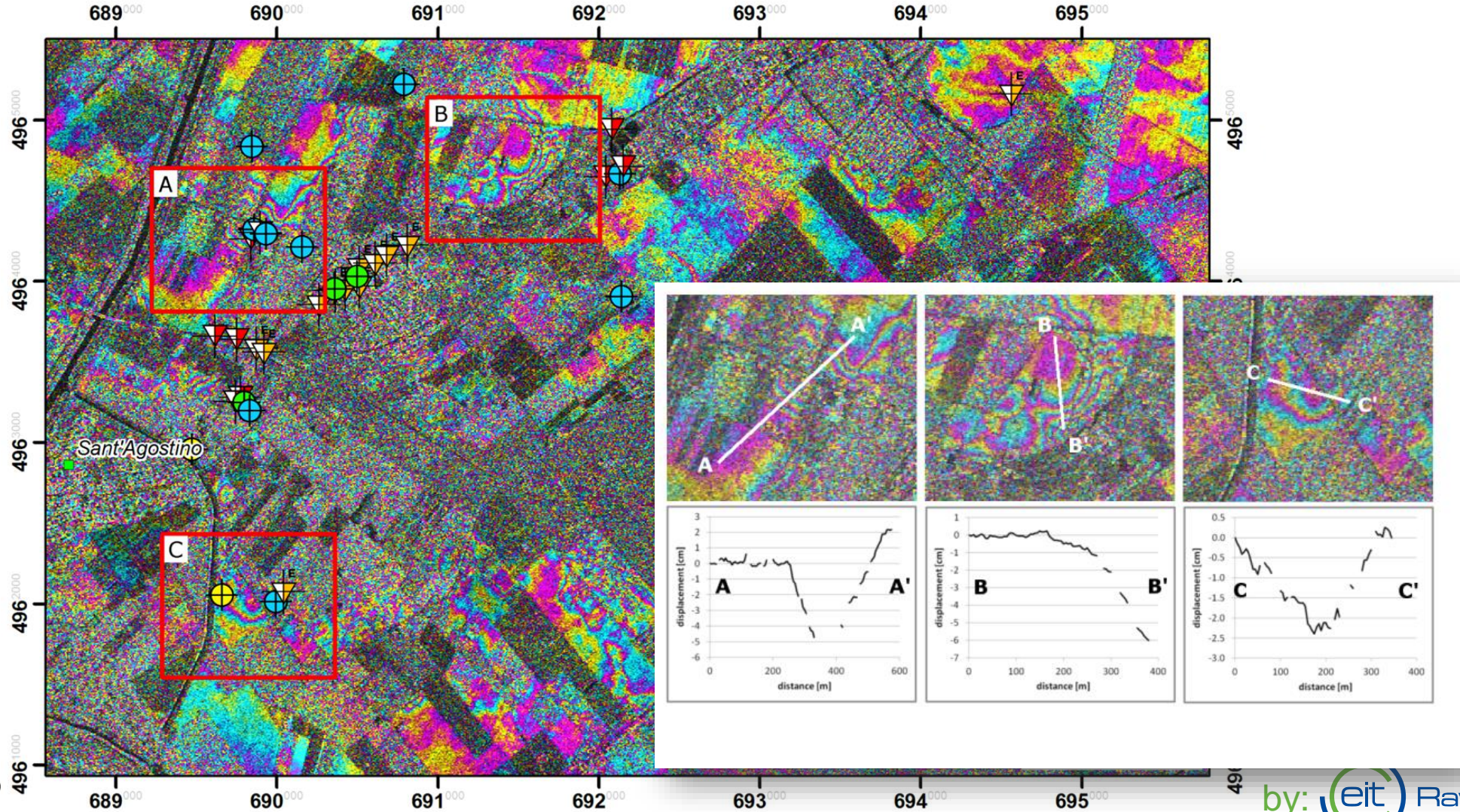
DGPV & InSAR



COSMO-SkyMed hi-res InSAR revealed DPGV for L'Aquila earthquake



Secondary effects of the earthquake: liquefactions



Multi-Temporal InSAR technique



This activity has received funding from the European Institute of Innovation and Technology (EIT), a body of the European Union, under the Horizon 2020, the EU Framework Programme for Research and Innovation

Multi-temporal InSAR technique

MT-InSAR techniques allow to discriminate the different components of the interferometric phase with high accuracy. Such methodologies allow to:

- model the phase trend due to the displacement and to evaluate the temporal and spatial evolution of the investigated phenomenon.
- retrieve the topographic component from the phase other than estimate the topographic residual hence an improvement in the movement modelling and the geocoding accuracy.
- estimate and removal of the atmospheric contribution.



Advantages & Disadvantages



- ✓ Using a huge number of SAR data provide a spatially dense (each interferogram) and temporally dense (time series) information.
- ✓ Detection of atmospheric artifacts spatially correlated and temporally uncorrelated.
- ✓ More accurate estimate and subsequent removal of orbital ramp and/or topographic residuals.
- ✓ Better velocity and displacement accuracy (until 1mm/yr).
- ✓ Possibility to work in low or high resolution.
- Expensive computational time for the processing.
- Wide storage space needed on hard-disk (not true for all the techniques).
- Needed tuning of a large number of parameters during the processing.
- Needed of at least 20-25 SAR images to obtain solid results.



Fieldworks of MT-InSAR techniques

Recently the use of InSAR has been addressed to the study of slow surface movements aiming to detect possible precursors of natural disasters.

Therefore as monitoring the evolution of phenomena through time and with very short displacement rates (few mm/yr) cannot be provide by standard InSAR, new approaches have been developed.

Multitemporal InSAR techniques dealing with a huge number of SAR images are now available. These can provide a dense temporal repetition interval and reduce the atmospheric and speckle effects.



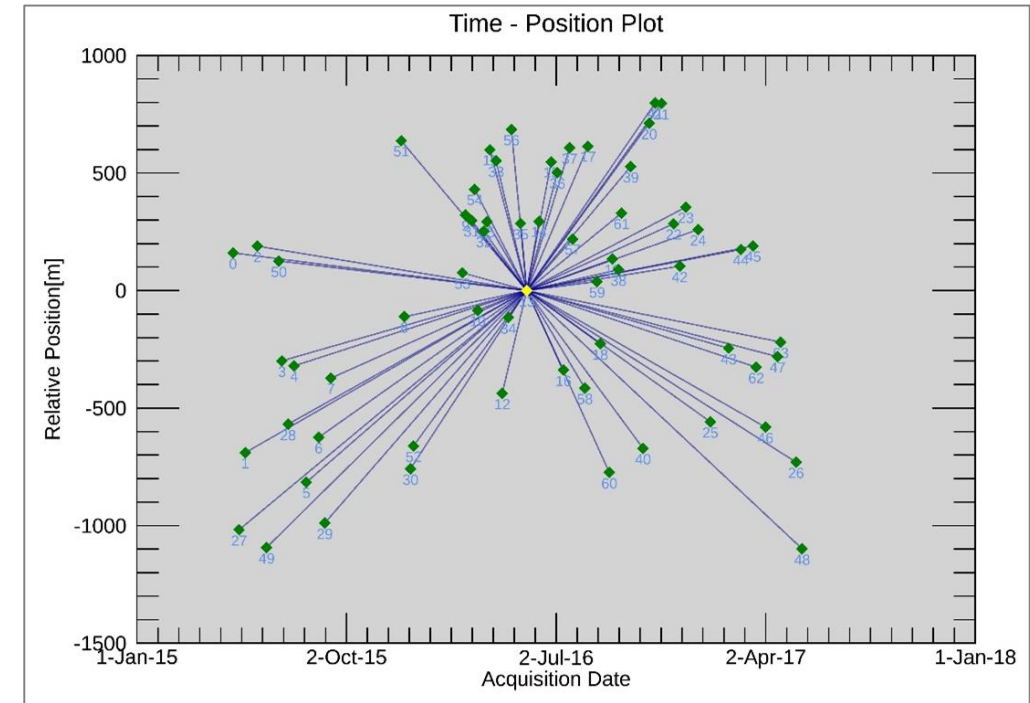
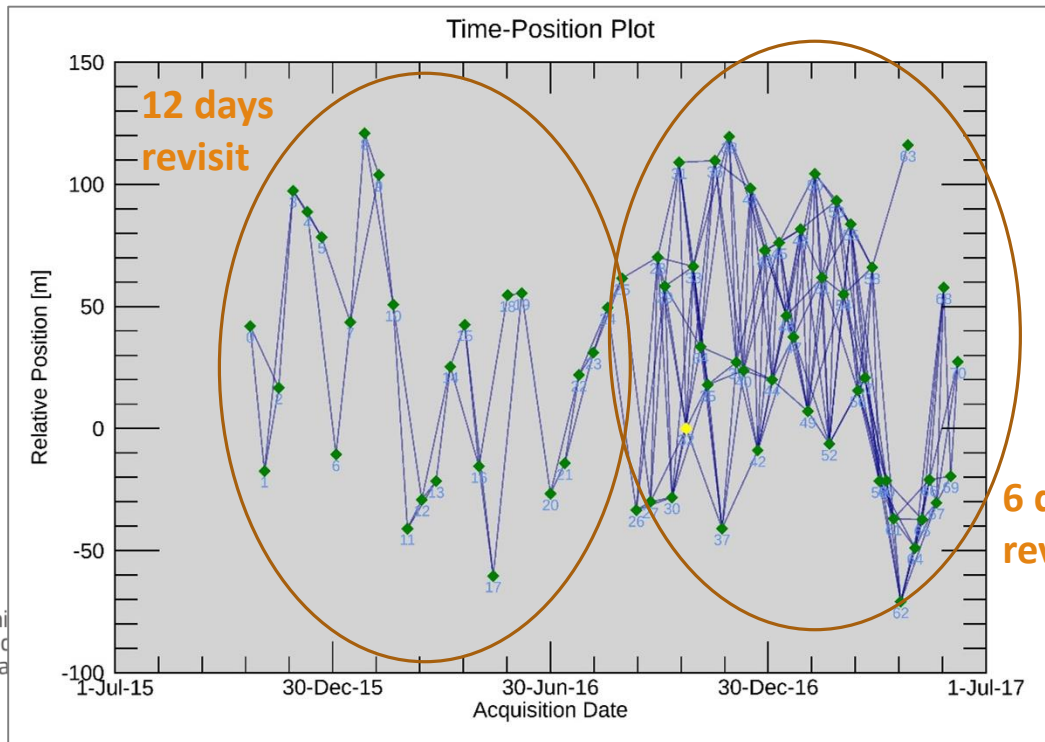
Multi-temporal InSAR technique

Two main categories of methods:

- Distributed Scatterers (DS), e.g. The SBAS method → all scatterers within the resolution cell
- Point Scatterers (PS), e.g. PS → single scatterer within the resolution cell, i.e. sub-pixel point

And two approaches of InSAR stack use:

- Single Master Reference 
- Multiple Masters (or multi-baseline)



Multi-temporal InSAR technique

How can we exploit the large dataset of SAR images available today??

A number of advanced InSAR techniques have been developed since 20 years ago:

- PS and SqueeSAR from POLIMI
- SBAS from CNR-IREA
- IPTA from GAMMA Remote Sensing
- PSP from E-GEOS
- STAMPS from Stanford University
-and many other

There are usually named as

PSI techniques – Persistent Scatterers Interferometry





RawMaterials

Connecting matters

The Permanent Scatterers (PS) technique

PSs are stable points selected in the intensity SAR images.

Advantages:

- Estimating and removing atmospheric effects;
- High accuracy displacement detection;
- Identification of the single PS.

Disadvantages

- A minimum number of SAR acquisitions needed;
- 20 PS/km² at least;
- Problems with very fast movements.



This activity has received funding from the European Institute of Innovation and Technology (EIT), a body of the European Union, under the Horizon 2020, the EU Framework Programme for Research and Innovation

Supported by:  RawMaterials
Connecting matters

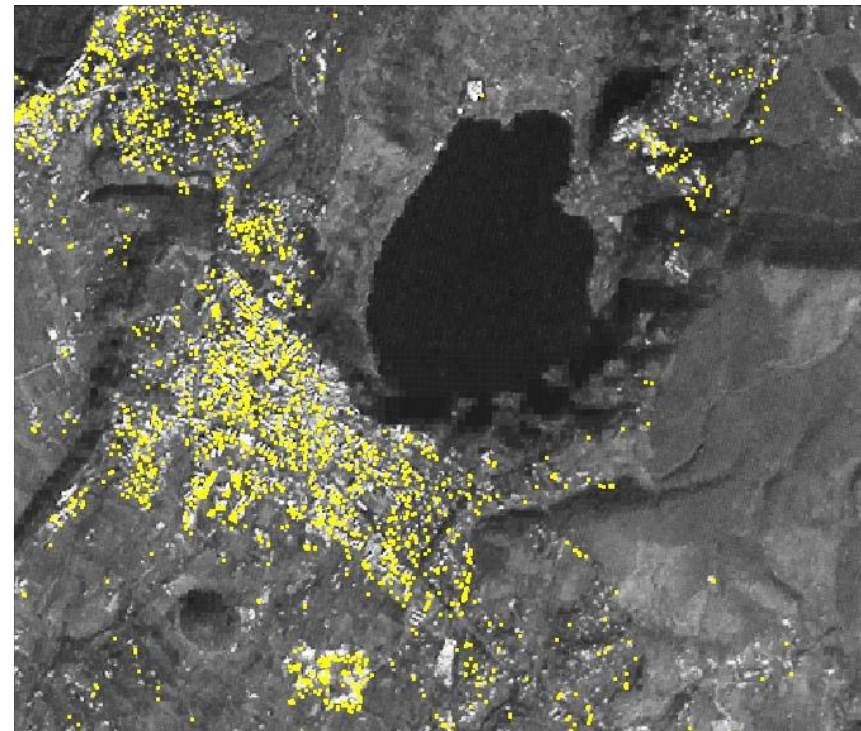
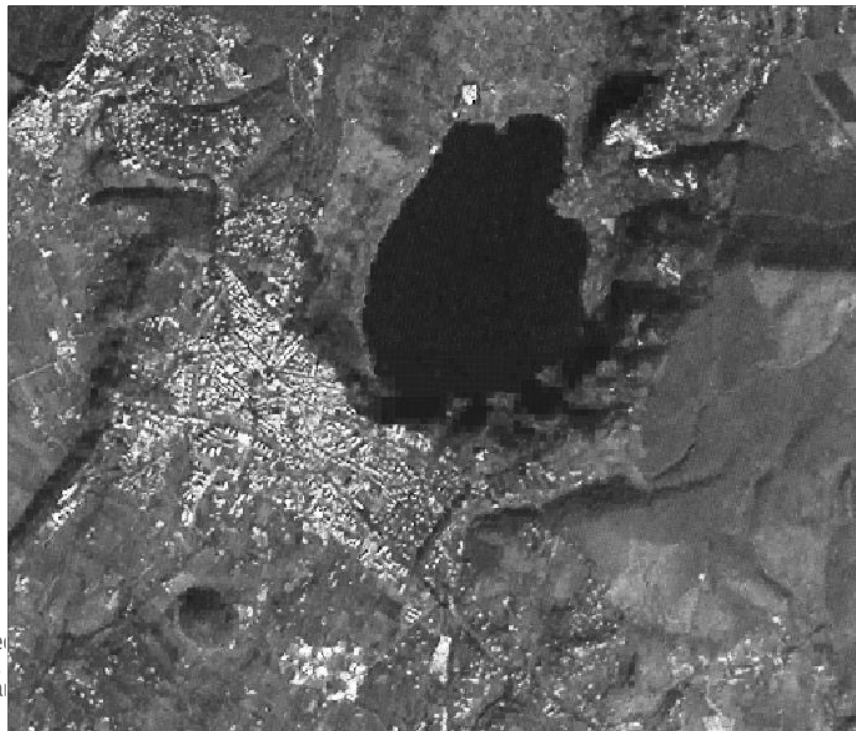
The Permanent Scatterers technique

- They are an extremely effective tool for monitoring deformation phenomena of the Earth's surface, based on the use of time series of SAR images.
- The processing originates from a statistical study of the images, which leads to the selection of a set of scatterers particularly suitable for estimating ground movement. These targets can coincide with single points or with distributed targets and are characterized by high phase stability, which allows to overcome most of the limitations related to conventional DInSAR analysis.
- In the case of single points we speak of Point Scatterers, in the second case of diffuse scatterers. The former gave rise to a series of techniques called Persistent Scatterers (PS, Ferretti et al., 2001), the latter to the Small Baseline subset technique (SBAS, Berardino et al., 2002).



The Permanent Scatterers technique

The PS grid can be imagined as a dense network of natural GPS (Global Positioning System) stations, characterized by a temporal data update frequency and an extremely high spatial density of measurement points (in urban areas 100-300 PS / km²).



The Permanent Scatterers technique

From a series of SAR images, only the points (PS) that maintain phase stability in all (or in a percentage) of the acquisitions are selected.

The phase data processing for each PS allows you to reconstruct the displacement of the point for each acquisition.

Main advantages

- estimation and removal of atmospheric disturbance
- identification of the single PS
- estimation of velocities (accuracy ~ mm / year)
- high spatial density of the PS in inhabited areas
- high accuracy of topographic information (~ 2 m)

Disadvantages:

- need for at least 20 SAR acquisitions
- minimum density PS (~ 20 per sq km)
- difficulty in identifying rapid motions (earthquakes, landslides ...)

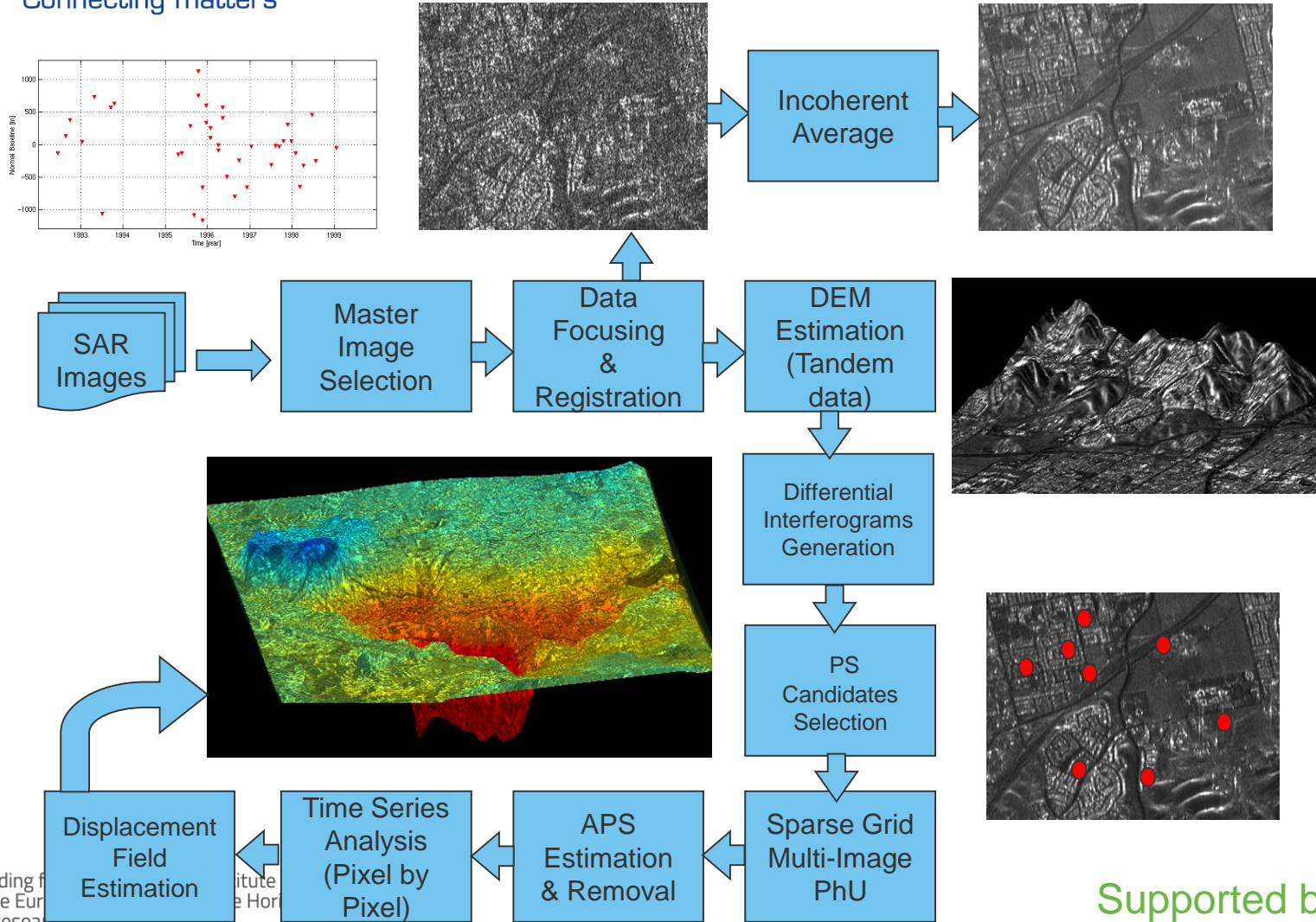




RawMaterials

The Permanent Scatterers technique

Connecting matters



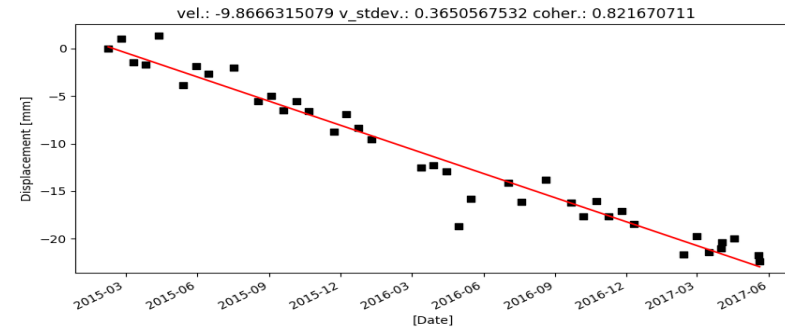
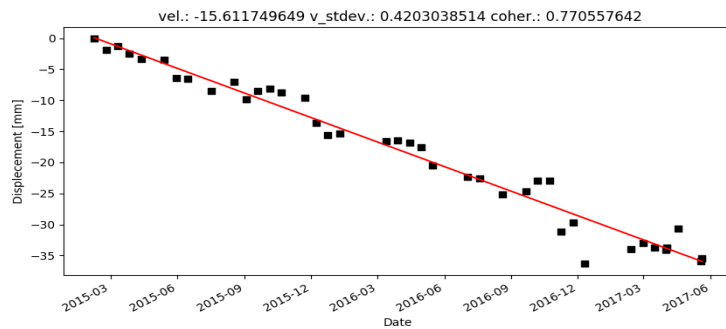
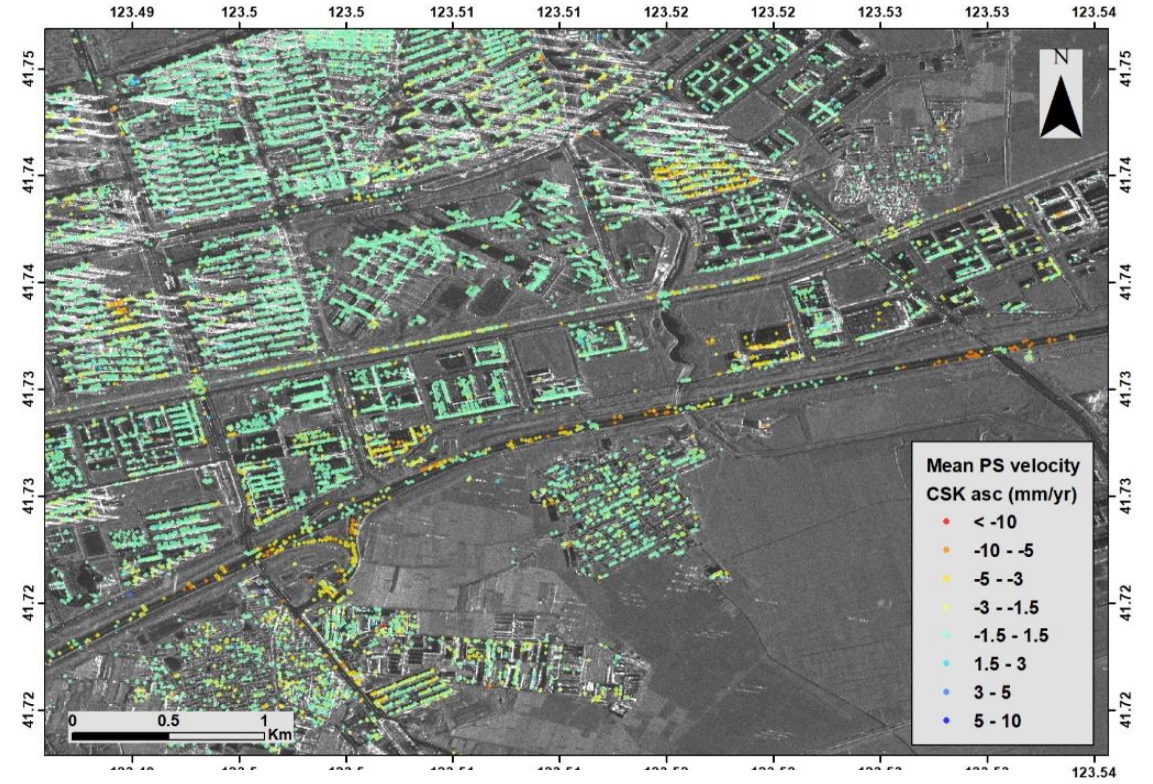
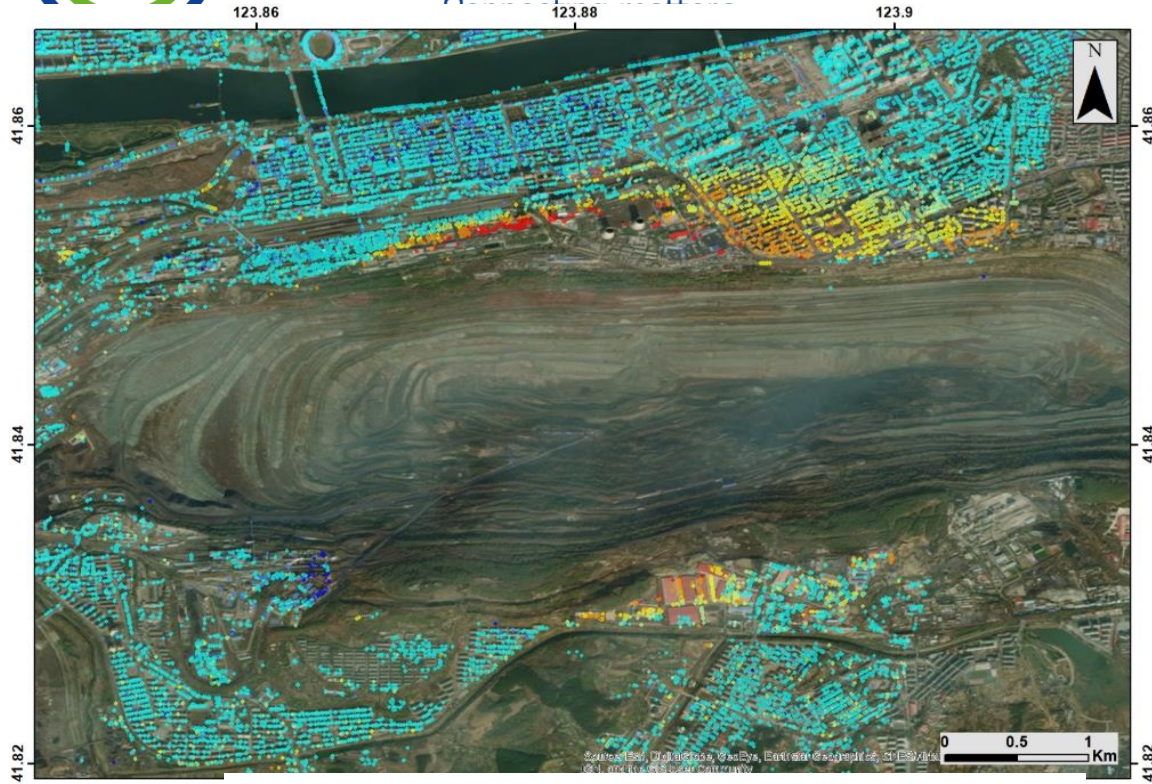
This activity has received funding from the European Union's Horizon 2020 research and innovation programme under grant agreement No 101019715.

The Permanent Scatterers technique

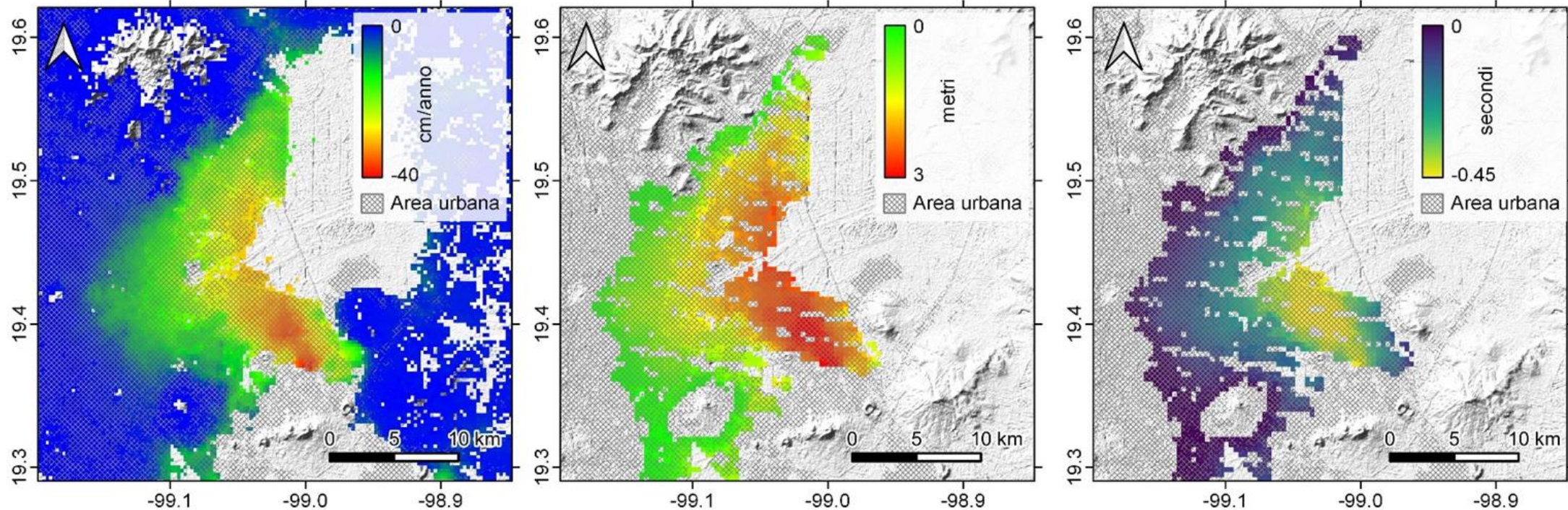
- The analysis with the PS basically provides deformation measurements along the line of sight of the sensor.
- The retrieved surface motion is always relative to a point of the image taken as reference.
- The information associated with each PS is finally geocoded in order to assign to each target a pair of coordinates expressed in the geographical reference system of the DEM used during the processing chain.
- Ease of integration of the data obtained in a GIS environment so to be able to carry out a complete analysis of the obtained information (validation, comparison, interpretation, etc.)



Subsidence in open pit mine



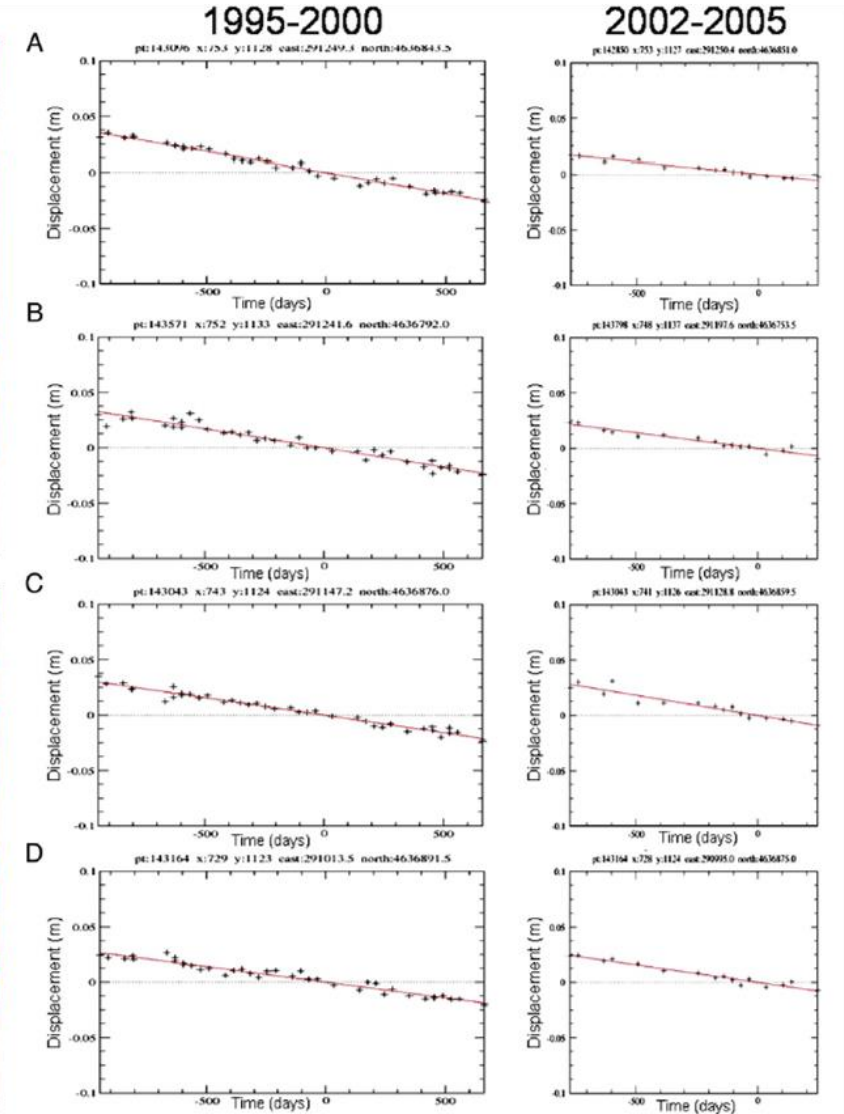
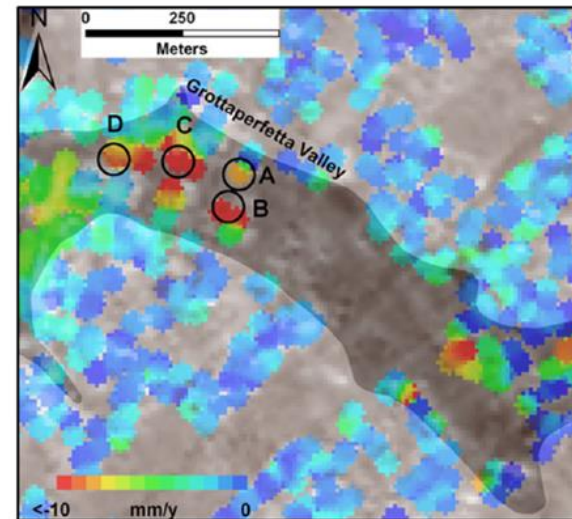
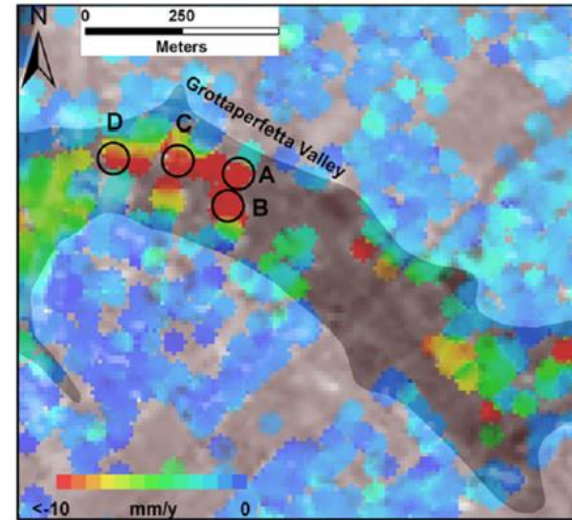
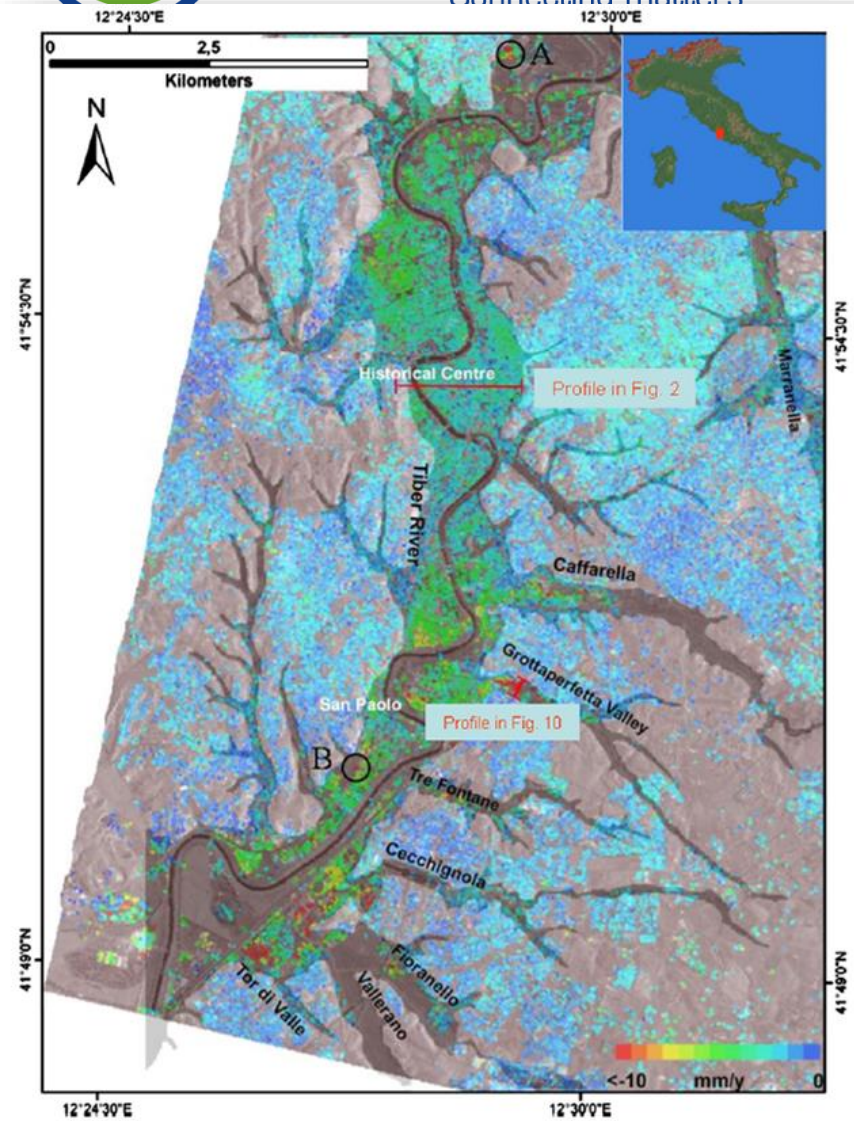
Subsidence in Mexico City



The annual rate of soil compaction has been studied in Mexico City and allowed the calculation of the soft-soil thickness changes. Through the modelling of such changes by means of geotechnical data, we can estimate the change in the soft soil resonant period during the observed period, and consequently infer the changes in the seismic response of the soil for a better characterization of seismic hazard at local scale

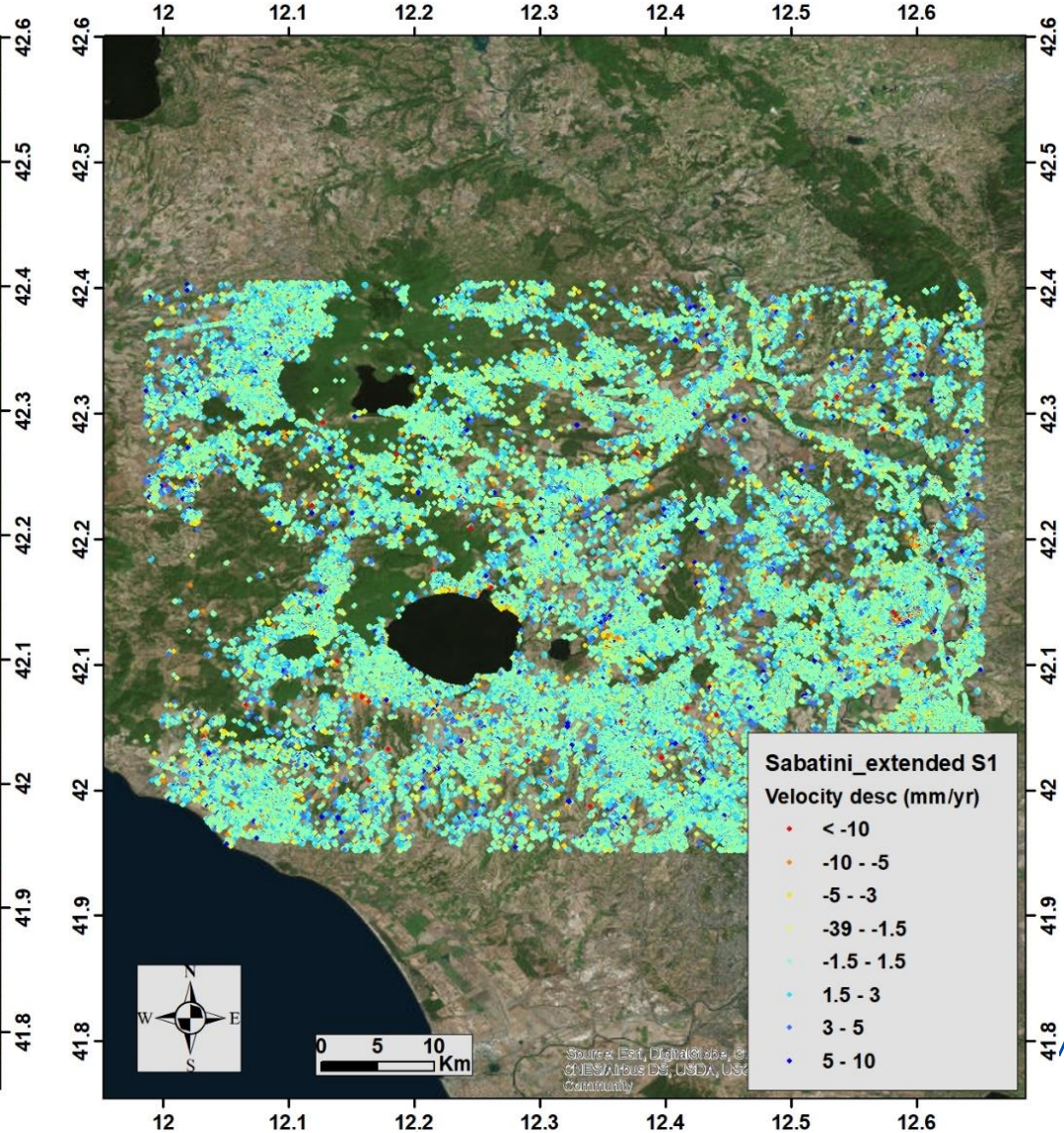
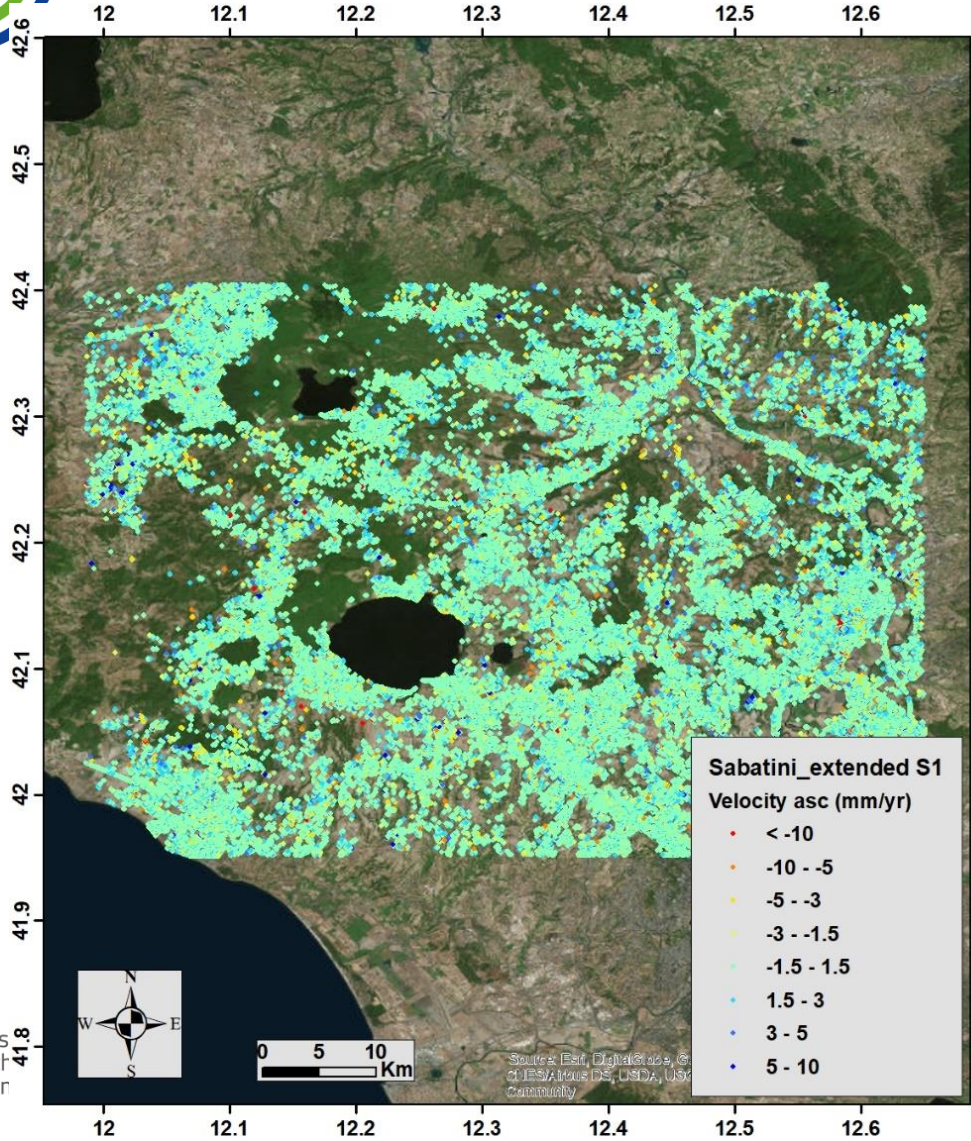


Subsidence in Rome





Ground velocity maps at Alban Hills (Rome)



Thank you for your attention

